ESL-TR-91-11

PHOTOIONIZATION IN COLLISION COMPLEXES

E. A. WALTERS, J. S. NIMITZ,
D. L. ARNEBERG, J. T. CLAY, JR.,
M. H. WALL, M. V. WILLCOX,
R. E. TAPSCOTT, AND J. R. GROVER

NEW MEXICO ENGINEERING RESEARCH INSTITUTE
UNIVERSITY OF NEW MEXICO
ALBUQUERQUE, NM 87131-1376

DECEMBER 1991

FINAL REPORT

MAY 1989 - OCTOBER 1990

APPROVED FOR PUBLIC RELEASE:
DISTRIBUTION UNLIMITED

AIR FORCE ENGINEERING & SERVICES CENTER
ENGINEERING & SERVICES LABORATORY
TYNDALL AIR FORCE BASE, FLORIDA 32403

NOTICE

The following commercial product (requiring Trademark ®) is mentioned in this report. Because of the frequency of usage, the trademark was not indicated.

HY-STOR 207

The following product (requiring Copyright ©) is mentioned in this report. Because of the frequency of usage, the copyright was not indicated.

NMERI HALOCARBON DATABASE

If it becomes necessary to reproduce any segment of this document containing any of these names, this notice must be included as part of that reproduction. Mention of the products listed above does not constitute Air Force endorsement or rejection of this product, and use of information contained herein for advertising purposes without obtaining clearance according to existing contractual agreements is prohibited.

NOTICE

PLEASE DO NOT REQUEST COPIES OF THIS REPORT FROM HQ AFESC/RD (ENGINEERING AND SERVICES LABORATORY). ADDITIONAL COPIES MAY BE PURCHASED FROM:

NATIONAL TECHNICAL INFORMATION SERVICE
5285 PORT ROYAL ROAD
SPRINGFIELD, VIRGINIA 22161

FEDERAL GOVERNMENT AGENCIES AND THEIR CONTRACTORS REGISTERED WITH DEFENSE TECHNICAL INFORMATION CENTER SHOULD DIRECT REQUESTS FOR COPIES OF THIS REPORT TO:

DEFENSE TECHNICAL INFORMATION CENTER
CAMERON STATION
ALEXANDRIA, VIRGINIA 22314

REPORT DOCUMENTATION PAGE	Form Approved OMB No. 0704-0188

1. AGENCY USE ONLY (Leave blank)	2. REPORT DATE	3. REPORT TYPE AND DATES COVERED
	December 1991	Final

4. TITLE AND SUBTITLE

PHOTOIONIZATION IN COLLISION COMPLEXES

5. FUNDING NUMBERS

F29601-C-87-0001

6. AUTHOR(S)

E. A. Walters, J. S. Nimitz, D. L. Arneberg, J. T. Clay, Jr., M. H. Wall, M. V. Willcox, R. E. Tapscott, and J. R. Grover

7. PERFORMING ORGANIZATION NAME(S) AND ADDRESS(ES)

New Mexico Engineering Research Institute
University of New Mexico
Albuquerque, New Mexico 87131-1376

8. PERFORMING ORGANIZATION REPORT NUMBER

SS 2.11(2)

9. SPONSORING/MONITORING AGENCY NAME(S) AND ADDRESS(ES)

Engineering and Services Laboratory
Air Force Engineering and Services Center
Tyndall Air Force Base, Florida 32403-6001

10. SPONSORING/MONITORING AGENCY REPORT NUMBER

ESL-TR-91-11

11. SUPPLEMENTARY NOTES

12a. DISTRIBUTION/AVAILABILITY STATEMENT	12b. DISTRIBUTION CODE

13. ABSTRACT (Maximum 200 words)

The overall objective of this effort was to determine the potential roles of van der Waals complexes of dioxygen, hydrocarbon fuel, and halon molecules in combustion and extinguishment. This study provides insights into the reactions between the fire extinguishant CF_3Br and the dominant flame free radicals H, O, and OH. Molecular complexes of halon/dioxygen, halon/hydrocarbon, and hydrocarbon/dioxygen were generated by expansion of gas mixtures through a supersonic nozzle. These complexes then underwent dissociative photoionization followed by mass spectrometric analysis. Photoion yield curves were analyzed to characterize fragmentation processes and energy states. Thermodynamic properties of the clusters and fragments were measured. No evidence of interaction of CF_3Br with H atoms was found. Studies of frozen collision complexes offer a powerful method for elucidating the initial steps of reaction chemistry. Small heteroclusters were prepared, relative number densities of neutrals were determined, kinetic energy distributions of fragment ions were measured, and the first reported analysis of clusters in a ternary molecular beam was carried out. The results of these experiments have many potentially significant implications for development of alternative fire suppression agents.

14. SUBJECT TERMS	15. NUMBER OF PAGES
Complexes, Clusters, Halon, Fuel, Oxygen, Radical, Mechanism, Extinguishment	16. PRICE CODE

17. SECURITY CLASSIFICATION OF REPORT	18. SECURITY CLASSIFICATION OF THIS PAGE	19. SECURITY CLASSIFICATION OF ABSTRACT	20. LIMITATION OF ABSTRACT
UNCLASSIFIED	Unclassified	Unclassified	Unclassified

NSN 7540-280-5500

Standard Form 298 (Rev. 2-89)
Prescribed by ANSI Std 239-18

EXECUTIVE SUMMARY

A. OBJECTIVE

The overall objective of this effort was to determine the potential roles of van der Waals complexes of dioxygen, hydrocarbon fuel, and halon molecules in combustion and extinguishment, and to determine whether energy transfer from dioxygen to hydrocarbons provides a mechanism for maintenance of combustion reactions.

B. BACKGROUND

The remarkable flame-suppressant ability of CF_3Br has yet to be explained satisfactorily. Reactions between CF_3Br and the flame free radicals (H, OH, and O) that participate in the chain-branching reaction

$$H + O_2 \rightarrow O + OH$$

may be very important for extinguishment. In this effort studies of complexes between CF_3Br and precursors of the free radicals O, OH, and H were initiated.

C. SCOPE

The scope of this task involved the generation of molecular complexes of halon/dioxygen, halon/hydrocarbon, and hydrocarbon/dioxygen by expansion of gas mixtures through a supersonic nozzle source followed by dissociative photoionization of the complex. The complexes were photodissociated with tunable vacuum ultraviolet light, and the photoion yield curves were analyzed to characterize the fragmentation processes and energy states. For the dioxygen/fuel complexes, photoion yield curves were compared with photoabsorption spectra of free dioxygen to determine the probability and time scale of electronic energy transfer.

D. METHODOLOGY

Two separate pieces of equipment were used. One was the molecular beam apparatus at the University of New Mexico. The other was the Brookhaven National Laboratory molecular beam apparatus used in conjunction with the vacuum ultraviolet synchrotron ring at the National Synchrotron Light Source.

E. TEST DESCRIPTION

In both apparatuses, samples from a supersonic beam of molecular clusters were passed through a photoionization source, then into a mass spectrometer. Molecules and ions resulting from the reactions were identified by their characteristic mass spectral patterns.

F. RESULTS

The thermodynamic properties of several clusters involving halon, fuel, and oxygen molecules were measured. Halon fragments formed during reactions induced by photoionization of these clusters were observed, and the thermodynamic properties of these fragments were measured. The results of the experiments reported in this study have potentially significant implications for identification of alternative fire suppression agents. New concepts for extinguishment methods and needed research directions are proposed.

G. CONCLUSIONS

This study has provided informative insights into the reactions between the fire extinguishant CF_3Br and the dominant flame free radicals H, O, and OH. The most important conclusions are the following:

(1) Little evidence that CF_3Br interacts with either O or OH radicals has been found. Potential fire extinguishants are compounds that will trap either of these radicals efficiently.

(2) The very low C-Br bond energy in the CF_3Br^+ ion suggests that some Br may enter flames from CF_3Br^+. The means of forming CF_3Br^+ or similar cations in flames should be explored.

(3) CF_3Br has been shown to react with H atoms. This reaction is found in the case of dissociative photoionization of clusters and in the metal hydride reduction of CF_3Br.

(4) Kinetic energy distributions of fragment ions of dissociative photoionization events can be measured. Detailed analysis of the results may show how to apply the method to systems involving halons.

(5) Since the high stability of and thermodynamic preference for CF_3^+ may be a strong driving force in the extinguishment process, a more thorough examination of this extinguishment mechanism should be conducted.

(6) Small heteroclusters can be prepared in supersonic-nozzle expansions and the relative number densities of the neutrals can be determined.

(7) Analysis of clusters in a ternary molecular beam has been carried out for the first time.

(8) Cluster growth in free-jet expansions cannot be described by a model based on near-equilibrium processes.

(9) Studies of frozen collision complexes, i.e., weakly bound or van der Waals complexes, offer a powerful method for learning about initial steps of reaction chemistry.

This approach should continue to yield worthwhile information about the mechanisms of reactions of halons, CFCs, HCFCs, and other small molecules.

H. RECOMMENDATIONS

Since it appears possible that ions of extinguishants may be extremely important, a search for compounds with lower ionization potential than CF_3Br and possessing a weak C-Br (or C-X, where X is a halogen or other leaving group) bond in the ion should be conducted. It is likely that such compounds will have relatively short tropospheric lifetimes, thus contributing to reduced ODP and GWP.

A search for compounds that trap either O or OH radicals should be conducted. For example, a molecule such as CF_3CH_2ONO will decompose readily at flame temperatures to give CF_3, CH_2O, and NO. NO reacts with either O or OH and may therefore serve as the radical trap, turning off the flame propagation step. Furthermore, this class of compounds should have short atmospheric lifetimes. The toxicity questions, however, remain. Other families of compounds with similar chemical properties exist, e.g., substituted hydroperoxides, and should be investigated.

Since these results point to the importance of a very stable carbonium ion, CF_3^+ in this case, a search should be conducted for molecules containing other groups that can form stable carbonium ions (e.g., allylic, tertiary, or benzylic groups).

PREFACE

This report was prepared by the New Mexico Engineering Research Institute (NMERI), University of New Mexico, Albuquerque, New Mexico 87131-1376, under contract F29601-87-C-0001, for the Engineering and Services Laboratory, Air Force Engineering and Services Center, Tyndall Air Force Base, Florida 32403-6001. This work was also supported in part under contract DE-AC-02-76CH0016 with the U. S. Department of Energy, Division of Chemical Sciences, Office of Basic Energy Sciences.

This report summarizes work accomplished at NMERI between May 1989 and October 1990. The HQ AFESC/RDCF Project Officer was Capt. John R. Floden. Jonathan S. Nimitz was the principal investigator. Special thanks go to Faye Whittington for her efforts in assembling the materials presented herein.

The report has been reviewed by the Public Affairs Officer (PA) and is releasable to the National Technical Information Service (NTIS). At NTIS it will be available to the general public, including foreign nationals.

JOHN R. FLODEN, Capt, USAF
Project Officer

NEIL H. FRAVEL, Lt Col, USAF
Chief, Engineering Research Division

L. M. WOMACK
Chief, Air Base Fire Protection
and Crash Rescue Systems Branch

FRANK P. GALLAGHER, Col, USAF
Director, Engineering and Services
Laboratory

(The reverse of this page is blank.)

TABLE OF CONTENTS

LIST OF FIGURES

LIST OF FIGURES
(CONTINUED)

LIST OF TABLES

LIST OF ABBREVIATIONS

AP	appearance potential
APT	Advanced Protection Technologies
KAFB	Kirtland Air Force Base
AFB	Air Force Base
UNM	University of New Mexico
CERF	Civil Engineering Research Facility
CFC	chlorofluorocarbon
FC	fluorocarbon
FTIR	Fourier transform infrared
FWHM	full width at half maximum height
GWP	global warming potential
HCC	hydrochlorocarbon
HCFC	hydrochlorofluorocarbon
HFC	hydrofluorocarbon
ID	inside diameter
IP	ionization potential
ir	infrared
NMERI	New Mexico Engineering Research Institute
NSLS	National Synchrotron Light Source
ODP	ozone depletion potential
PIE	photoionization efficiency
USAF	United States Air Force
UV	ultraviolet
VUV	vacuum ultraviolet

LIST OF SYMBOLS

In the text, many of these symbols are followed by a subscript and/or superscript.

C_p	specific heat at constant pressure
C_v	specific heat at constant volume
D	dissociation energy
e	electron charge
E	energy
h	Planck's constant
k	Boltzmann constant
m	mass in amu units
T	temperature
P	pressure
υ	frequency

SECTION I
INTRODUCTION

A. OBJECTIVE

The overall objective of this effort was to determine the potential roles of van der Waals complexes of dioxygen, hydrocarbon fuel, and halon molecules in combustion and extinguishment, and to determine if energy transfer from dioxygen to hydrocarbons provides a mechanism for maintenance of combustion reactions.

B. BACKGROUND

The remarkable flame-suppressant ability of CF_3Br has yet to be explained satisfactorily. Reactions between the flame free radicals (H, OH, and O) which participate in the chain-branching reaction

$$H + O_2 \rightarrow O + OH \qquad [1]^1$$

and CF_3Br may be very important for extinguishment. In this effort, studies of complexes between CF_3Br and precursors of the free radicals O, OH, and H were initiated.

Recent investigations have indicated that halon fire-extinguishing agents may have a significant environmental impact owing to their potential to deplete stratospheric ozone. For that reason, the availability and use of halons may be restricted in the near future. Through the Halon Research Program, the Air Force is seeking alternative agents and technologies for fire extinguishment. An integral part of this program is basic research into combustion and extinguishment to aid in the development of new suppression concepts.

---

[1]For the convenience of the reader, reaction numbers are given in square brackets and equation numbers in parentheses.

Recently, a unique method for the generation and quantitative study of reactive intermediates has been developed. This method permits the characterization of molecular van der Waals complexes and their fragmentation products, which may be important in both combustion and extinguishment. The method consists of dissociative photoionization of weakly bound complexes formed in supersonic-nozzle expansions. Nonstatistical reactions can be induced by short wavelength (vacuum ultraviolet) radiation to give a wide variety of reactive intermediates, either cations or free radicals. Measurement of threshold energies for these processes permits precise determination of heats of formation and gives insight into reaction pathways. For example, irradiation of the benzene with a hydrogen chloride (C_6H_6 + HCl) complex under collisionless conditions leads to the formation of the Wheland intermediate for chlorination of benzene, $C_6H_6Cl^+$. This reaction requires the participation of a "solvent" molecule, so the complete process is correctly given by $(C_6H_6)_2HCl + h\upsilon \rightarrow C_6H_6Cl^+ + H + C_6H_6 + e^-$. Determination of the threshold energy, $E_{th} = (h\upsilon)_{th}$, for this reaction allows calculation of the heat of formation of $C_6H_6Cl^+$. Kinetic energy analysis of the product ion establishes the internal energy of $C_6H_6Cl^+$ as formed and clarifies the mechanism of formation of this cationic reaction intermediate.

The proper choice of complexing partners offers the possibility of the synthesis of free-radical intermediates and the precise determination of their thermodynamic properties. For example, the complex $(C_3H_5Br)_2$ dissociates to yield the unstable radical HBr_2, whose ground state properties can be studied. The use of fuels, oxygen, and halons in appropriate weak molecular complexes can, by the method of dissociative photoionization, lead to the production of important intermediates in combustion and extinguishment and will permit the identification of potential "solvation." It is important to establish such pathways because complex formation and solvent effects, even in gas-phase reactions, appear to be general phenomena.

In previous efforts experimental approaches to the study of the initial fire suppression reactions of halons were verified and preliminary experiments were conducted (References 1 and 2). Three experimental methods were examined:

(1) laser Raman spectroscopy, (2) isolation of products of an argon matrix followed by Fourier transform infrared spectroscopy, and (3) photoionization of molecular clusters followed by mass spectrometry. It was determined that photoionization mass spectrometry was the most effective of these techniques for studying the initial reaction of halons with free radicals. One system of a halon molecule (Halon 1301, CF_3Br) and a flame free-radical precursor (O_2) was carefully studied. Thermodynamic properties of the clusters and fragments were measured.

C. SCOPE

In this study the nature of the interactions among the following chemical species was examined: dominant flame free radicals (O, OH, and H), a hydrocarbon fuel (C_6H_6), its fluorinated analogue (C_6F_6), and a halon (CF_3Br). Experiments were carried out in which O and OH were generated inside small clusters in a molecular beam with the aid of short wavelength radiation. Reactions between H atoms and CF_3Br were surface reactions, and analysis was performed using FTIR spectroscopy. A device for determining the kinetic energy distribution of the fragment ions of cluster dissociative photoionization was designed, built, tested, and employed in a series of experiments. Thus, a wide range of chemical reaction possibilities was encompassed in a small number of individual experiments.

D. TECHNICAL APPROACH

Threshold photoionization data are used to characterize the output of a Ar/methanol/bromotrifluoromethane expansion. Fragment ion intensity versus source pressure is measured. Small, weakly bound clusters of CF_3Br (Halon 1301) with O_2 and CH_3OH were prepared in supersonic jets and studied by photoionization and dissociative photoionization using a photoionization mass spectrometer. The light source was a tunable vacuum ultraviolet (VUV) beam from the 750 MeV electron storage ring at the National Synchrotron Light Source, Brookhaven National Laboratory.

Phase I (Development of Experimentation Plan) included a review of the appropriate technology and development of a detailed plan for performing studies of the formation and fragmentation within dioxygen/hydrocarbon, halon/hydrocarbon, and dioxygen/halon complexes using dissociative photoionization techniques. The plan included studies of energy transfer and atomic rearrangement within dioxygen/hydrocarbon complexes.

Phase II (Performance of Photodissociative Experiments) involved the use of gas-expansion techniques to form complexes of halons, dioxygen, and hydrocarbon fuel, which were photolyzed to give dissociative fragments. Photoion yield curves through the wavelength regime in which photoionization occurs were obtained. Accurate photoion threshold measurements were performed. Experiments were conducted at both Brookhaven and UNM. The complexes examined include CF_3Br with CH_3OH (with methanol acting as an OH source), O_2 with benzene (a hydrocarbon fuel molecule), and CF_3Br with O_2 (in a continuation of studies using dioxygen as an oxygen atom source). An apparatus was designed and constructed at the University of New Mexico (UNM) to study the reactions of halon molecules with hydrogen atoms generated from a metal hydride.

Phase III (Analysis of Results) involved the analysis of the data obtained to characterize the complexes and photodissociative fragments observed. The results of these experiments yield information on the reactions of all three of the triad of major flame free radicals (O, OH, and H) with halons and also provide evidence for the mechanism by which halons disrupt flame free-radical reactions.

SECTION II
REVIEW OF PREVIOUS WORK

In previous efforts, experimental procedures for the characterization of the reactions and molecular products formed when halons enter flames were evaluated and verified. Initial studies using those procedures were performed. Three techniques were studied to compare their usefulness for determining the concentrations of chemical species in flames: laser Raman spectroscopy, matrix isolation Fourier-transform infrared spectroscopy, and photoionization mass spectroscopy. Laser Raman spectroscopy of hydrogen/oxygen flames extinguished with Halon 1301 provided identification of the principal flame species; however, this method was not effective in detecting minor species present in low concentrations. The Raman spectrum of the hydrogen molecule was used to calculate flame temperatures. The purpose of the matrix isolation experiments was to characterize the fragmentation patterns of Halons 1211, 2402, and 1301. The expected fragments and some stable molecules were observed. Of the three techniques, photoionization mass spectrometry was found to be the most promising method for characterizing the very early reactions occurring in flames. It was found that Halon 1211 does react with the free radical H, but the cross section of the overall process is small. No evidence was found for reactions between O atoms and either Halon 1211 or 1301. A database of fire suppression literature was developed and incorporated into the NMERI HALOCARBON DATABASE©.

One system of a halon molecule (Halon 1301, CF_3Br) and a flame free-radical precursor (O_2) was carefully studied. Thermodynamic properties of the clusters and fragments were measured.

Two separate pieces of equipment were used. One was the molecular beam apparatus at the University of New Mexico. The other was the Brookhaven National Laboratory molecular beam apparatus used in conjunction with the vacuum ultraviolet synchrotron ring at the National Synchrotron Light Source.

In both apparatuses, samples from a supersonic molecular beam of clusters of Halon 1301 and O_2 molecules were ionized by vacuum ultraviolet light in the ionizer of a mass spectrometer. Molecules and ions resulting from the reactions of CF_3Br and O_2 were identified by their characteristic mass spectral patterns and appearance potentials.

The thermodynamic properties of several halon fragments were measured. One striking result is that no oxygenated fragments of the halon molecule were observed.

The lack of oxygenated halon fragments may indicate that direct trapping of oxygen radicals by halon is not an important mechanism for flame extinguishment. The extremely weak C-Br bond in CF_3Br^+ suggests that Br atoms enter flames via the ion CF_3Br^+ rather than from CF_3Br itself. Some evidence indicates that the CF_3 portion of the halon molecule may have a more significant role in flame extinguishment than previously suspected.

Future work should direct attention to the two other members of the triad of flame free radicals, H and OH, and that the dissociative photoionization approach to weakly bound clusters of Halon 1301 and flame free-radical precursors be extended to H and OH precursors.

SECTION III
EXPERIMENTAL PROCEDURES

A. CLUSTERS OF O_2 WITH C_6H_6 OR C_6F_6

The dimers $C_6H_6 \cdot O_2$ and $C_6F_6 \cdot O_2$, and the mixed trimers of C_6H_6 and O_2 and of C_6F_6 and O_2, were studied by photoionization methods at line U-11. Although it has long been known that especially interesting interactions exist between oxygen and aromatic hydrocarbons and fluorocarbons, this is the first successful study of their gas-phase complexes.

The reactant systems to be studied were synthesized and made into molecular beams by collimation of free-jet expansions of mixtures of the reagent gases. The resulting molecular beams were mixtures of products. Substantial control of the beam composition was achieved by varying the proportions of the gases, nozzle pressure, and temperature, but it was not possible at this time to obtain a pure beam of any particular target cluster. Instead, it was necessary to make measurements on the mixtures and extract from these results the data specific to the species of interest. For this purpose, one must be able to analyze the composition of the beam. This proved to be a significant challenge, but good progress was made.

This work was carried out using the tunable photon beams of 350 to 1500 Å available from the monochromator at line U-11 of NSLS. The VUV photon beam is made to cross the molecular beam in the center of an ionizer containing the lens system that focuses the ions on the entrance aperture of a quadrupole mass spectrometer operated in the ion-counting mode. The apparatus is shown schematically in Figure 1. A detailed description of both the apparatus and the experimental technique has been given elsewhere (Reference 2). For the experiments described here, O_2 was bubbled through C_6H_6 or C_6F_6 at room temperature (23 °C), such that a constant head pressure of the mixed gases (O_2 + C_6H_6 or O_2 + C_6F_6) was maintained. This bubbling resulted in a mixture of constant composition in the head space. The mixture was then expanded through the jet at a pressure substantially below the head pressure. In the case of

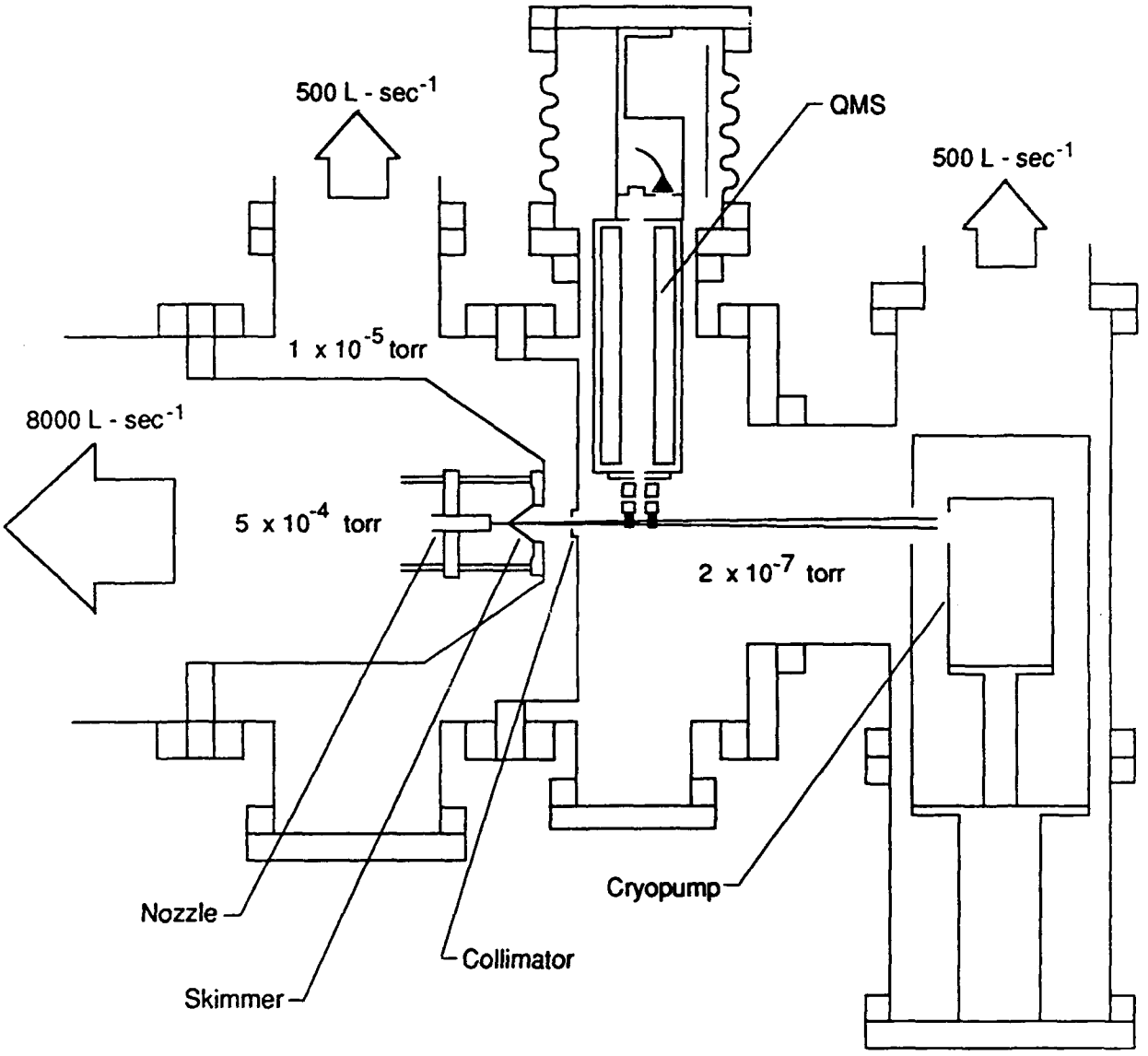

Figure 1. Schematic Drawing of Photoionization Mass Spectrometer.

O_2 + C_6H_6, the composition of the mixture in the head space was C_6H_6:O_2 of 1:127 at a head pressure of 3900 torr. The technique described below was used to determine the distribution of $C_6H_6 \bullet O_2$ clusters as a function of nozzle pressure, and an operating pressure of P = 1500 or 2500 torr was chosen for most of the photoion yield curve measurements. Under these conditions, the $C_6H_6 \bullet O_2$ cluster was dense enough to give reasonable signals, but trimer densities were low enough that their fragmentations did not contribute to the signal. The experiments for the O_2 + C_6F_6 system were carried out in a very similar manner, except that the nozzle pressure was P = 1500 torr at a head pressure of 4000 torr.

The procedure developed for establishing the relative density of heterodimers in molecular beams formed from free-jet expansions of gas mixtures has been described (Reference 3). It is based on the observation that, near threshold, the photoionization efficiency (PIE) function for the dissociative photoionization of the weak heterodimer A•B,

$$A \bullet B + h\upsilon \rightarrow A^+ + B + e \qquad [2]$$

increases rapidly with photon energy when the PIE function of A has a distinct step at the threshold for direct ionization (Reference 4). Thus, at a fixed photon energy in this region, the PIE amplitude of Reaction [2] is proportional to the density of A•B in the ionization volume. The simultaneous contribution of A^+ from dissociative ionization of the homodimer A•A is expected to be negligible, because of the characteristically high dissociation energies of homodimer ions (Reference 4). We have found the contribution PA^+ from dissociative ionization of A•A to be negligible in each of the systems investigated so far, including ethylene, 1,3-butadiene, and benzene. Since most of the A^+ ions observed during the actual measurement are generated by the direct ionization of monomeric A, the contribution to the A^+ signal from dissociative ionization is identified by the difference method described earlier (Reference 4) with the convenient modification that measurements at only two photon energies are required. One ($h\upsilon$ = E_o) must lie between the ionization energy of A and the threshold for dissociative ionization of A•B, and the other well above the threshold for dissociative ionization.

To achieve the requisite selectivity for heterodimers, however, the higher energy must be below the thresholds for producing A^+ from trimers and larger clusters. The experiments described here were carried out utilizing the tunable vacuum ultraviolet beam available at the National Synchrotron Light Source, Brookhaven National Laboratory.

B. CLUSTERS OF CF_3Br WITH CH_3OH

The experiments reported here were performed as described previously by photoionization mass spectrometry applied to molecular beams collimated from jet expansions (References 4 and 5). The source of ionizing radiation was a tunable vacuum ultraviolet beam provided by the National Synchrotron Light Source at Brookhaven National Laboratory. The composition of the expanding mixture was maintained at $Ar:CF_3Br:CH_3OH$ = 293:28:1 by bubbling a 10.5:1 $Ar:CF_3Br$ mixture at 2200 torr through methanol temperature-controlled at -21.5 °C. This composition roughly maximized yields of $(CF_3Br{\bullet}CH_3OH)^+$ ions with the nozzle (diameter = 0.0100 cm) at room temperature. The effective beam temperatures, calculated from an empirical expression (Reference 5), ranged from 11 to 4 K for nozzle pressures of 200 to 1200 torr, assuming that C_P/C_v = 1.48 for the mixed gases at 300 K, based on literature C_P values for CH_3OH (Reference 6) and CF_3Br (Reference 7). A lithium fluoride filter 0.2 cm thick was used to eliminate second-order radiation.

Cluster number densities in the molecular beam were determined as a function of nozzle pressure as described elsewhere (Reference 8). The ion used as a probe for each cluster, the threshold energy of the ion, and the energy used for the measurement are presented in Table 1. Note that measurement energies 0.36 to 0.54 eV (8 to 12 kcal/ mol) above the corresponding thresholds were used, which improved signal intensities considerably compared to the intensities available at 0.15 eV above threshold, where the measurements are usually made. At the same time, the contributions from fragmentation of larger clusters, tested for as in Reference 5, were still negligible for all the clusters considered. CH_3^+ was used to establish the pressure dependence of monomeric CH_3OH, and for monomeric CF_3Br the probe was CF_3^+. No complex ions

TABLE 1. PROBE IONS USED, THEIR IONIZATION AND APPEARANCE POTENTIALS, AND PHOTON ENERGIES CHOSEN FOR THE MEASUREMENTS.

Cluster	M/e used	Photon Energy, eV		
		Threshold	Used for measurement	Used for background
$(CH_3OH)_2$	33	10.160	10.552	10.039
$(CH_3OH)_3$	65	10.13	10.507	9.999
$CF_3Br{\cdot}CH_3OH$	180	10.76	11.302	10.716
$CF_3Br(CH_3OH)_2$	212	10.12	10.507	9.999
$(CF_3Br)_2$	298	11.23	11.587	10.972

incorporating Ar were seen in inventory scans taken at 584 Å and 700 Å. More definitively, no CF_3Br^+ ion ascribable to fragmentation of clusters (at 584 Å) could be detected via the search method described in Reference 5. This absence of complexes with argon is likely due to inefficient cooling in the presence of a third body with many internal energy modes. Finally, the measured relative number densities of the monomers and clusters in the range of 200- to 500-torr nozzle pressure, plus the constraint provided by the nozzle pressure dependence of total CH_3OH and CF_3Br, were used to solve for the relative proportions of the individual clusters.

C. REACTIONS OF CF_3Br WITH METAL HYDRIDES

Twenty-five grams of the alloy $LaNi_{4.7}Al_{0.3}$, HY-STOR 207 (Aldrich), were placed in a stainless steel chamber and evacuated to 0.050 torr for 12 hours. The alloy was activated by filling the chamber to 6000 torr with dry H_2. The pressure soon dropped and eventually reached an equilibrium at about 700 torr. The chamber was quickly evacuated to 375 torr and charged to 1220 torr with CF_3Br (Great Lakes Chemical Co.). This system was heated to 50 °C for 14 hours and allowed to cool to room temperature. The pressure at room temperature had increased to 1450 torr. The heating and cooling cycle was repeated two more times. After the third cycle, the room temperature pressure was 1710 torr. The condensible gases were trapped in a clean stainless steel cylinder (750 mL) by immersing one end of the cylinder in liquid N_2. After warming, a

10 cm long ir absorption cell with NaCl windows to room temperature, the cell was filled to 300 torr with the gaseous products on a vacuum line. The infrared absorption spectrum was then recorded on a Bomem FTIR spectrophotomer.

D. ION-KINETIC ENERGY ANALYZER

The problem being addressed is illustrated in Figure 2. In this example, the weakly bound complex $(C_6H_6)_2HCl$ experiences dissociative photoionization with the $C_6H_6Cl^+$ product ion appearing at 837 Å and shorter wavelengths:

$$(C_6H_6)_2HCl + h\upsilon \rightarrow C_6H_6Cl^+ + C_6H_6 + H + e \qquad [3]$$

In the proposed mechanism, translationally hot $C_6H_6Cl^+$ is generated. Many other mechanisms are possible, so a measurement of the kinetic energy of $C_6H_6Cl^+$ can yield detailed mechanistic information. Simple ion-kinetic energy analysis is complicated by the fact that the ions are generated with the kinetic energy of the molecular beam carrying them through the ionization region of the mass spectrometer (Figure 3). To overcome the beam kinetic energy problem, a kinetic energy filter was developed to replace both the customary extraction and focusing lens elements of the quadrupole mass spectrometer. The conceptual design consisted of lens elements with a series of annular slots at appropriate potentials, so that only ions in a certain kinetic energy range would be transmitted. The conceptual design was given realistic form using the program SIMION. Parameters from the SIMION model were used to construct the gold-plated stainless-steel lens shown in Figure 4. Voltages to the elements were supplied from an external source, and the values were chosen from extensive model calculations with SIMION, so that ions of a specific kinetic energy were transmitted. A range of kinetic energies was scanned at a given molecular mass.

The device was calibrated by preparing mixtures of known concentrations of Ar in He and expanding these through the nozzle under conditions such that the Ar kinetic energy could be calculated. Ar^+ (m/e 40) was then detected, and the kinetic energies

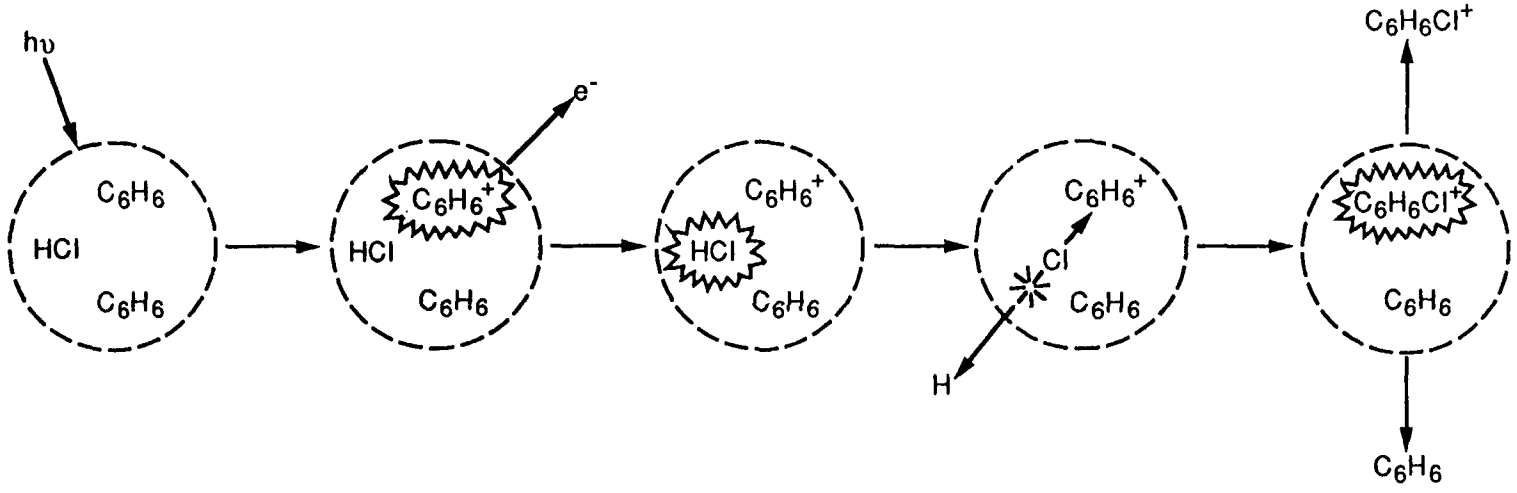

Figure 2. Proposed Mechanism for the Dissociative Photoionization of the Weakly Bound Complex $(C_6H_6)_2HCl$.

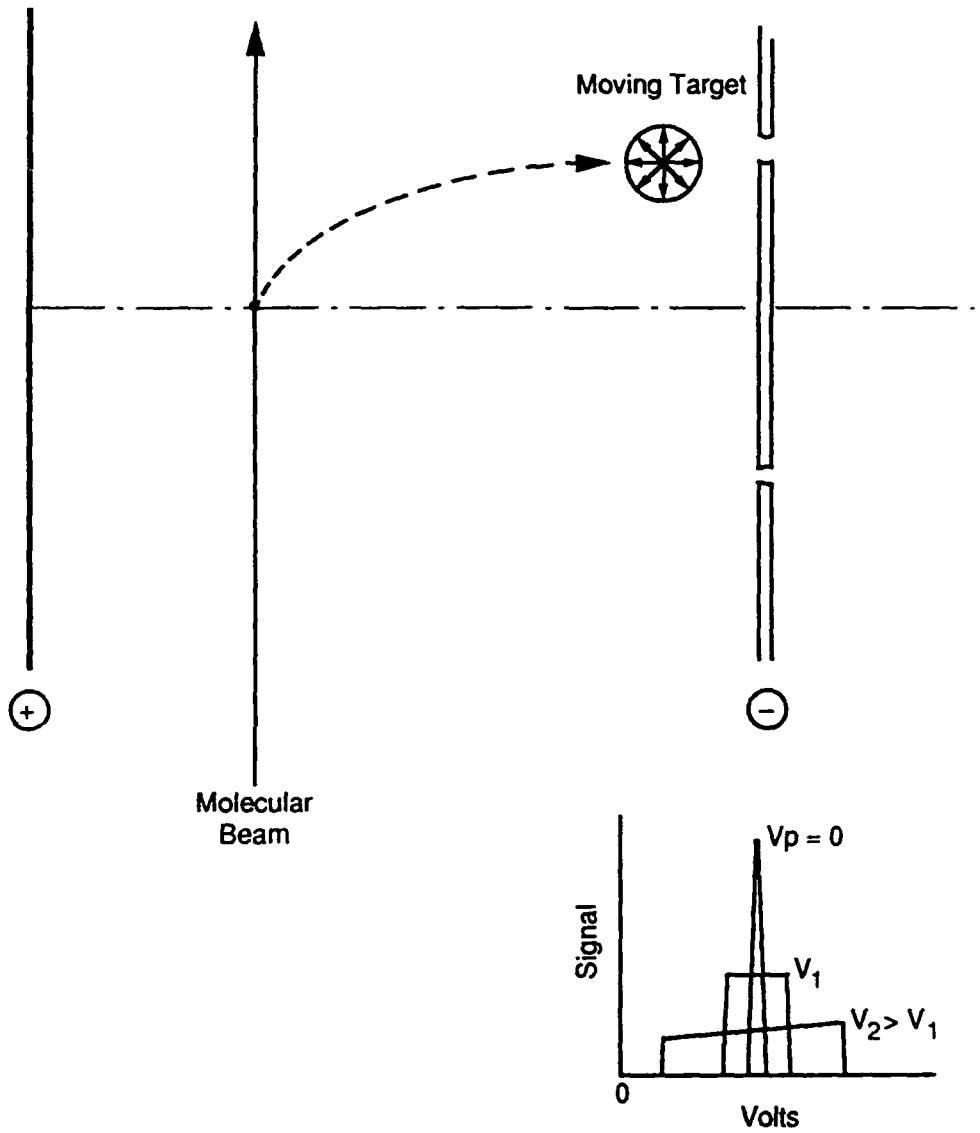

Figure 3. Behavior of Ions Generated from a Molecular Beam Passing Through the Ionization Region of a Mass Spectrometer. (Ions so produced have a component of translational energy in the direction of the molecular beam.)

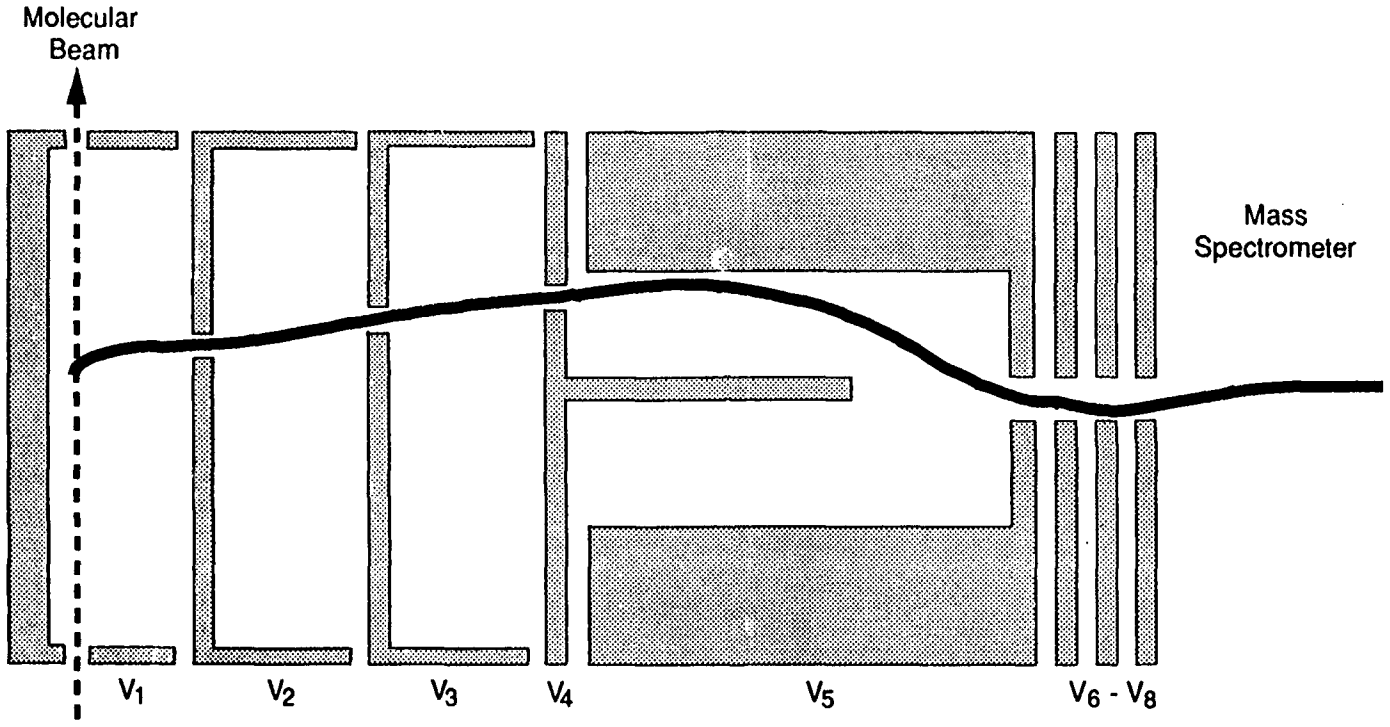

Figure 4. The Ion Kinetic Energy Lens. (Ionization by synchrotron radiation occurs in the molecular beam midway between the entrance and exit openings. The heavy line shows the calculated ion trajectory for optimum voltages of the lens elements.)

measured by the lens were compared with calculated kinetic energies from the expansion conditions. The results are shown in Figure 5.

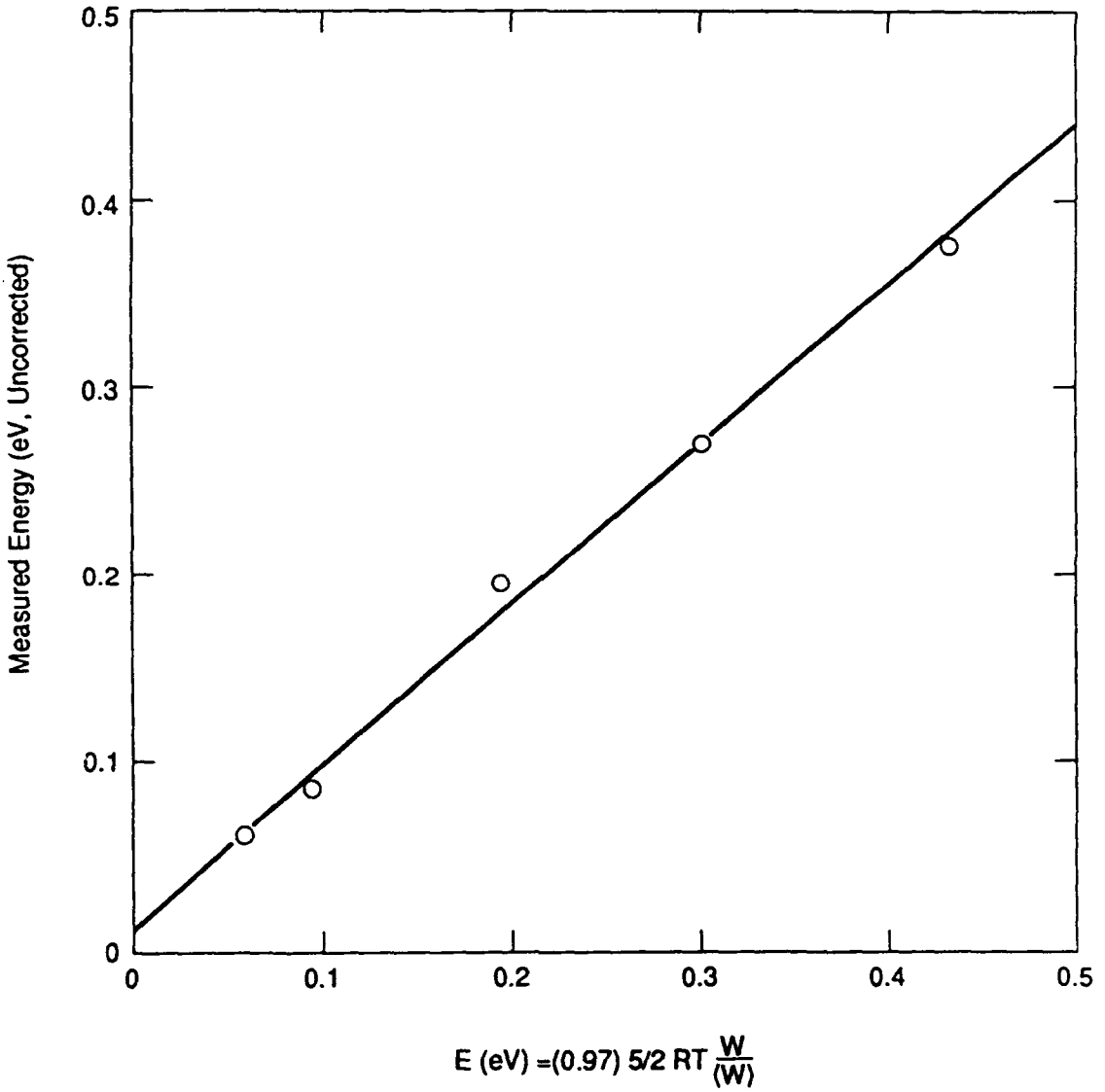

Figure 5. Measured Kinetic Energies of Ar^+. (Values were determined by the ion kinetic energy lens versus kinetic energies of Ar neutrals in Ar/He mixtures expanded through a 0.1-mm supersonic jet.)

SECTION IV
RESULTS AND DISCUSSION

A. O_2 PLUS C_6H_6 OR C_6F_6

When oxygen is dissolved in liquid benzene or substituted benzene, weak new features appear in the ultraviolet absorption spectrum that are not present in either constituent alone. These features consist primarily of a distinct red shift in the tail of the strong uv absorption band. These are explained as transitions to structures involving charge separation, such as

$$C_6H_6 \cdot O_2 + h\upsilon \rightarrow C_6H_6^+ \cdot O_2^- \qquad [4]$$

and called a "charge-transfer spectrum." The corresponding ground state complexes have not been isolated, so the charge-transfer absorptions are understood to take place during evanescent encounters between substrate oxygen. The dissociation energies are therefore very small, on the order of 1 kcal mol^{-1}, that is, not much different from thermal energy, kT, at room temperature.

The stable complex $C_6H_6 \cdot O_2$ at low temperature has been identified as a product of the free-jet expansion of a mixture of 99.7 percent oxygen and 0.3 percent benzene. It can be seen directly via its parent ion $C_6H_6 \cdot O_2^+$ and indirectly through the reaction

$$C_6H_6 \cdot O_2 + h\upsilon \rightarrow C_6H_6^+ + O_2 + e \qquad [5]$$

which is easily observed by subtraction of the photoionization efficiency function for the production of $C_6H_6^+$ (from pure benzene) from the corresponding function for the production of $C_6H_6^+$ (from the mixture expansion). The successful synthesis of $C_6H_6 \cdot O_2$ opens the way to the determination of its structure. Although these experiments do not contain direct structural information, they do provide benchmarks for quantum chemical calculations of these fluxional species. The photoion yield curve near the threshold of

$C_6H_6 \cdot O_2^+$ is shown in Figure 6. The threshold of $C_6H_6^+$ from clusters is shown in Figure 7.

Both the ionization potential of $C_6H_6 \cdot O_2$ and the appearance potential of $C_6H_6^+$ from $C_6H_6 \cdot O_2$ can be used to calculate the dissociation energies of both $C_6H_6 \cdot O_2$ and $(C_6H_6 \cdot O_2)^+$, as shown in the energy diagram in Figure 8. The results are:

$$D_o^\circ(C_6H_6 \cdot O_2) = 1.20 \pm 0.45 \text{ kcal mol}^{-1} \quad (1)$$

$$D_o^\circ([C_6H_6 \cdot O_2]^+) = 2.86 \pm 0.48 \text{ kcal mol}^{-1} \quad (2)$$

Correction to room temperature gives

$$D_{298}^\circ(C_6H_6 \cdot O_2) = 0.5 \pm 0.5 \text{ kcal mol}^{-1} \quad (3)$$

in support of the observed nonisolability of the benzene-oxygen complex.

Autoionizing structures are conspicuous in the photoionization spectrum of $C_6H_6 \cdot O_2$, an example of which is described below. Indeed, that the ionization potential shown in Figure 7 is so well-marked is most likely due to autoionization in the threshold region. The fact that these structures can be seen at all is very surprising, and it is important to understand the reason(s) why they are visible. Further work in this direction is needed. Figure 9 shows the autoionization structures in $(C_6H_6 \cdot O_2)^+$.

The dissociative rearrangement of $(C_6H_6 \cdot O_2)^+$ to produce $C_6H_6O^+$ has been observed. In this process, the strong O-O bond is broken while the weak C_6H_6--O_2 bond survives. As depicted below, nozzle pressure studies show that at 500 Å the yield of $C_6H_6O^+$ closely parallels the production of trimers in the jet expansion, but that at 800 Å significant production from heterodimers is taking place. The first observable onset, at 14.2 eV, is far above the true threshold at 9.2 eV. Figure 10 shows dimer/$C_6H_6O^+$ and trimer/$C_6H_6O^+$ ratios versus nozzle pressure at 500 Å and 800 Å. Figure 11 shows the onset of $C_6H_6O^+$.

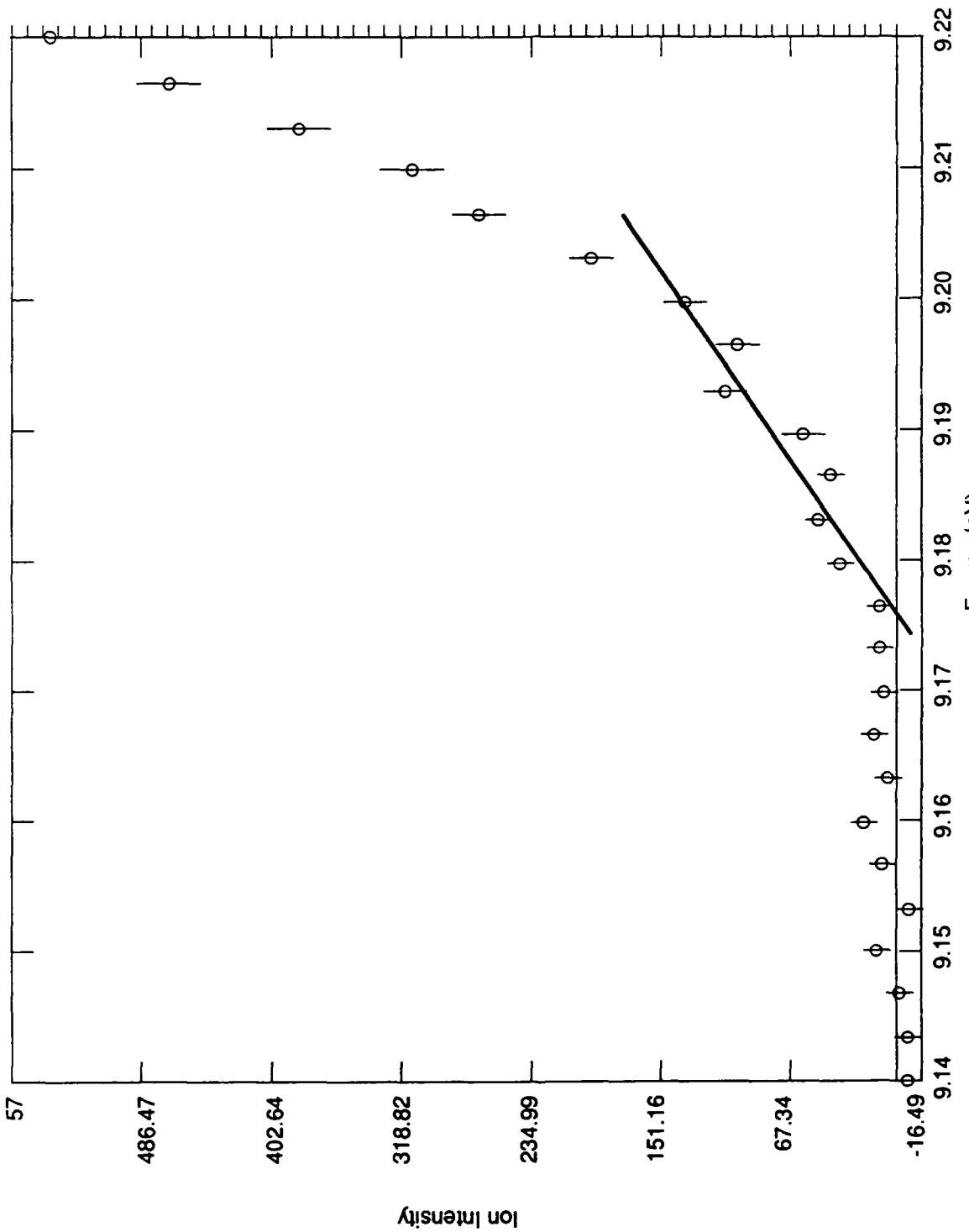

Figure 6. Threshold Region for $C_6H_6{\bullet}O_2 + h\upsilon \rightarrow (C_6H_6{\bullet}O_2)^+ + e.$

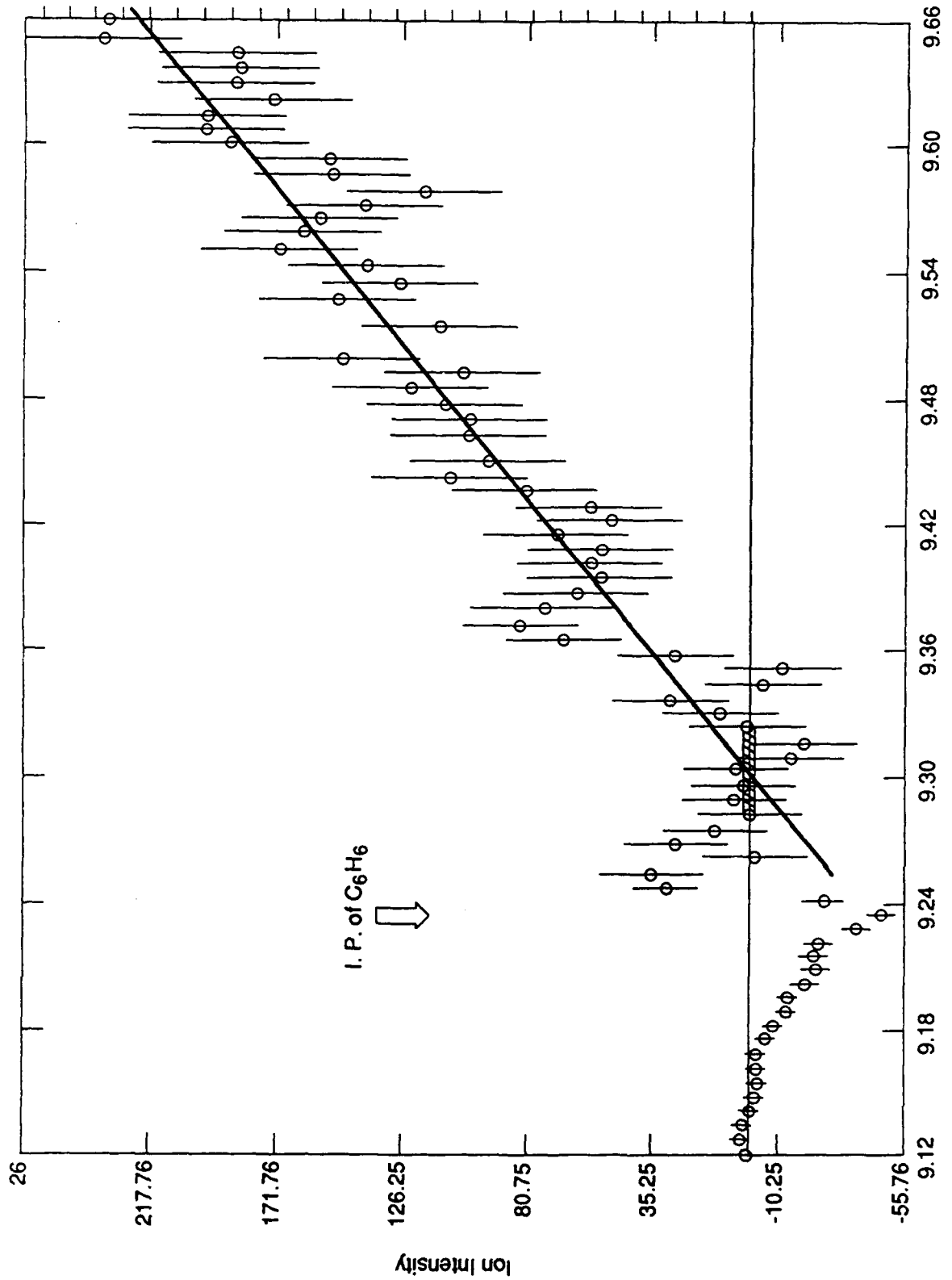

Figure 7. Ion Intensity Versus Energy for the Reaction $C_6H_6 \cdot O_2 + h\upsilon \rightarrow C_6H_6^+ + O_2 + e.$

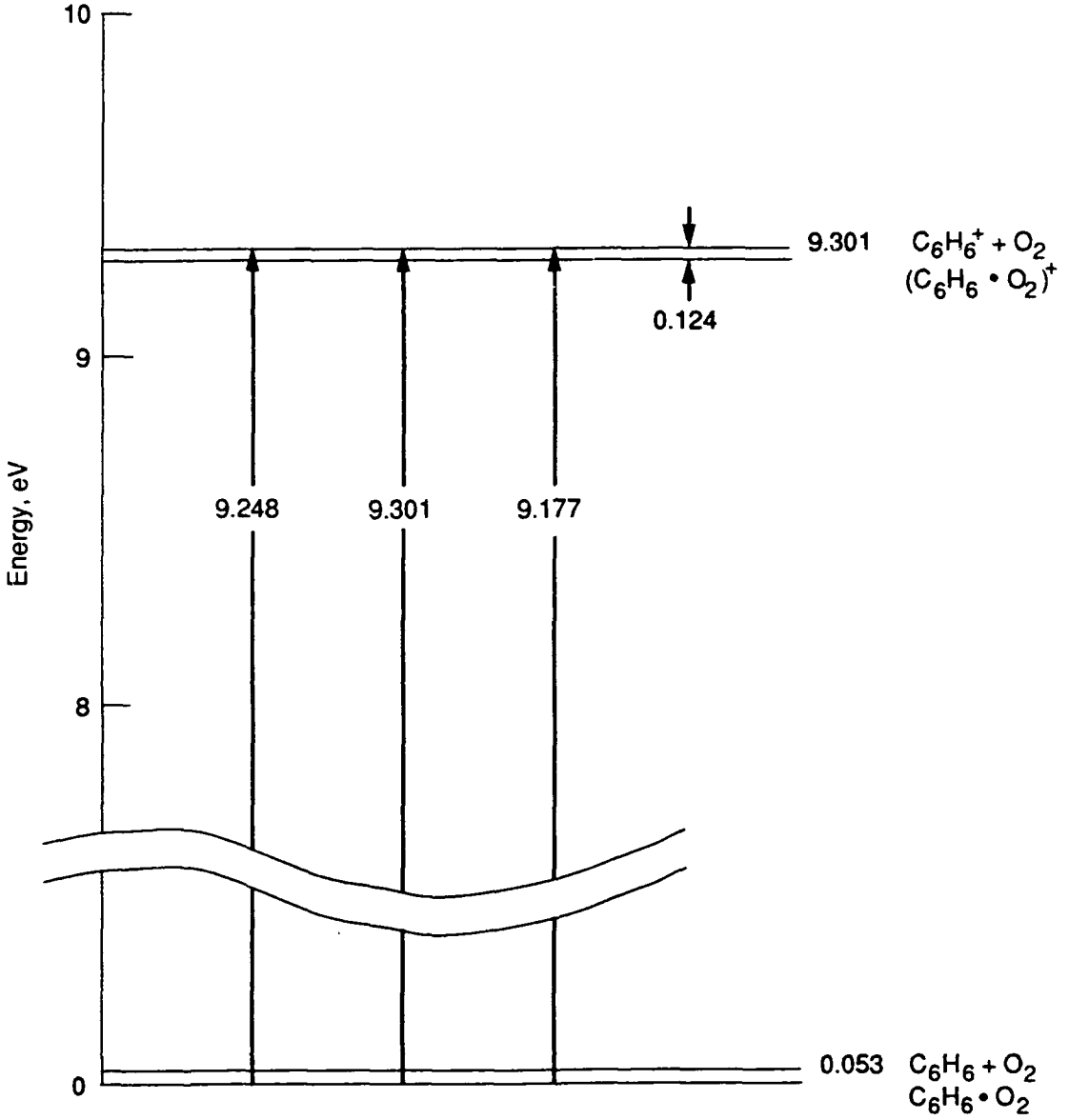

Figure 8. Energy Diagram in the $C_6H_6 + O_2$ System (in eV).

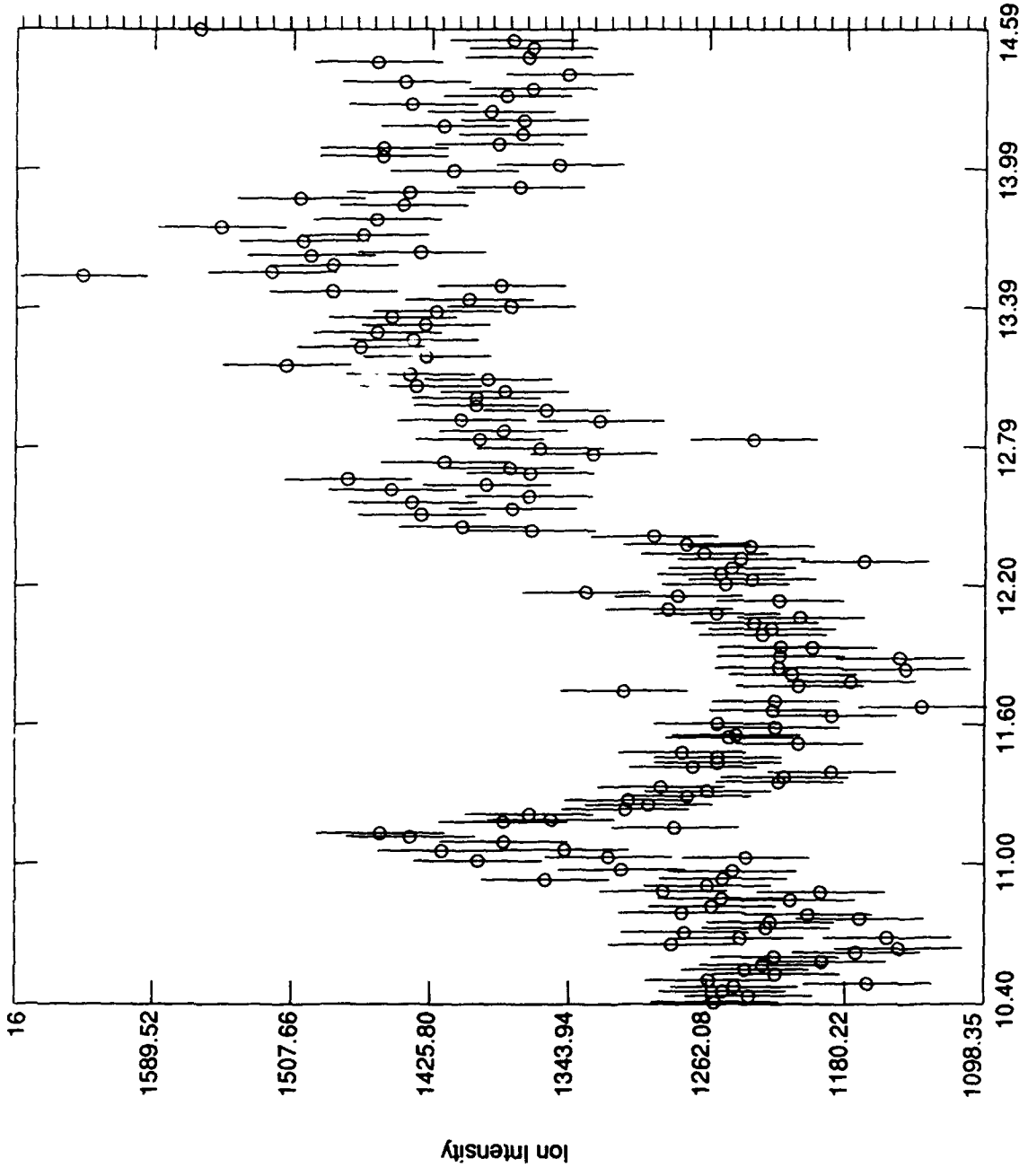

Figure 9. Autoionization Structure in $C_6H_6 \cdot O_2 + h\upsilon \longrightarrow (C_6H_6 \cdot O_2)^+ + e.$

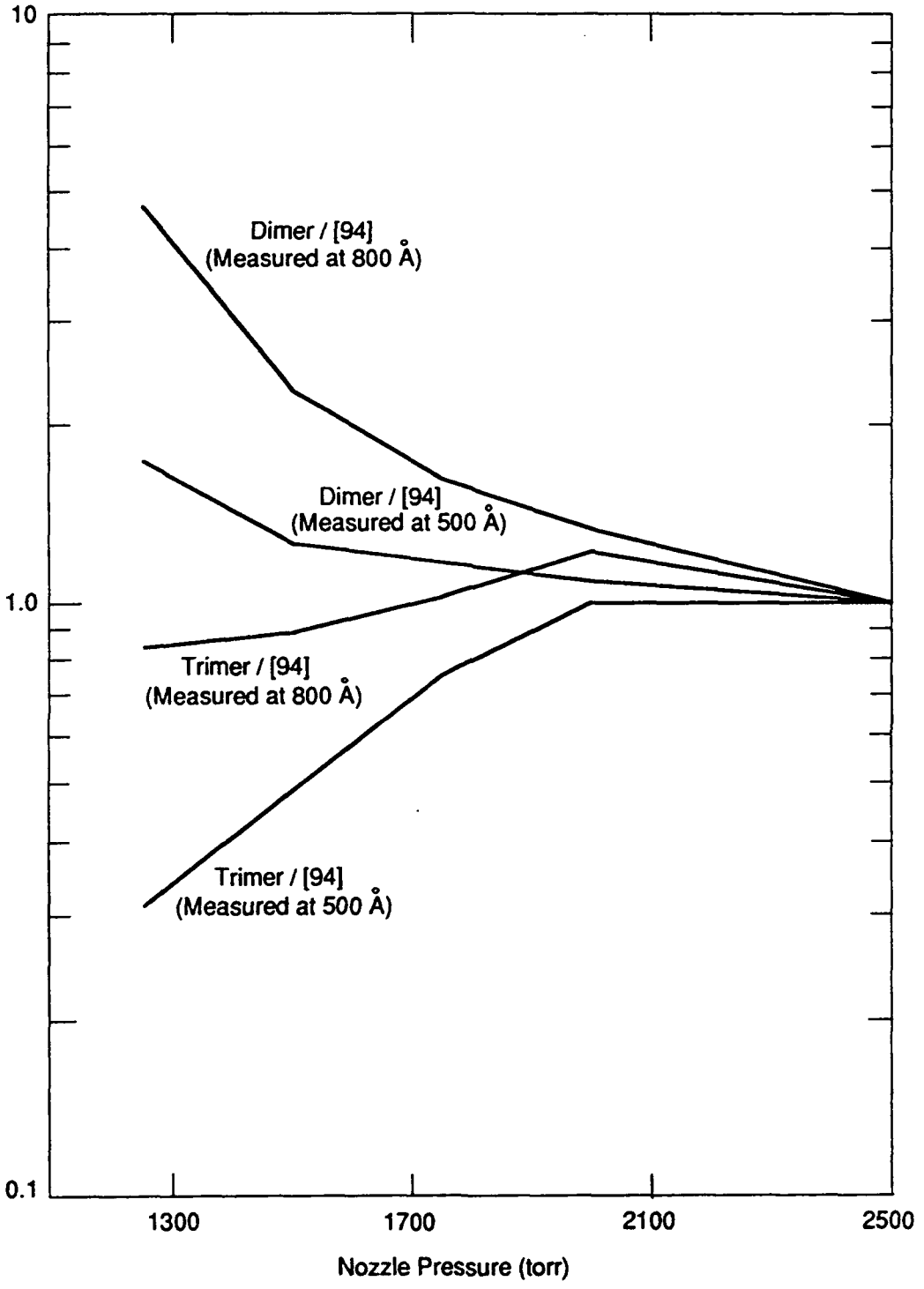

Figure 10. Comparison of Yield of $C_6H_6O^+$ with Beam Densities of Dimers and Trimers.

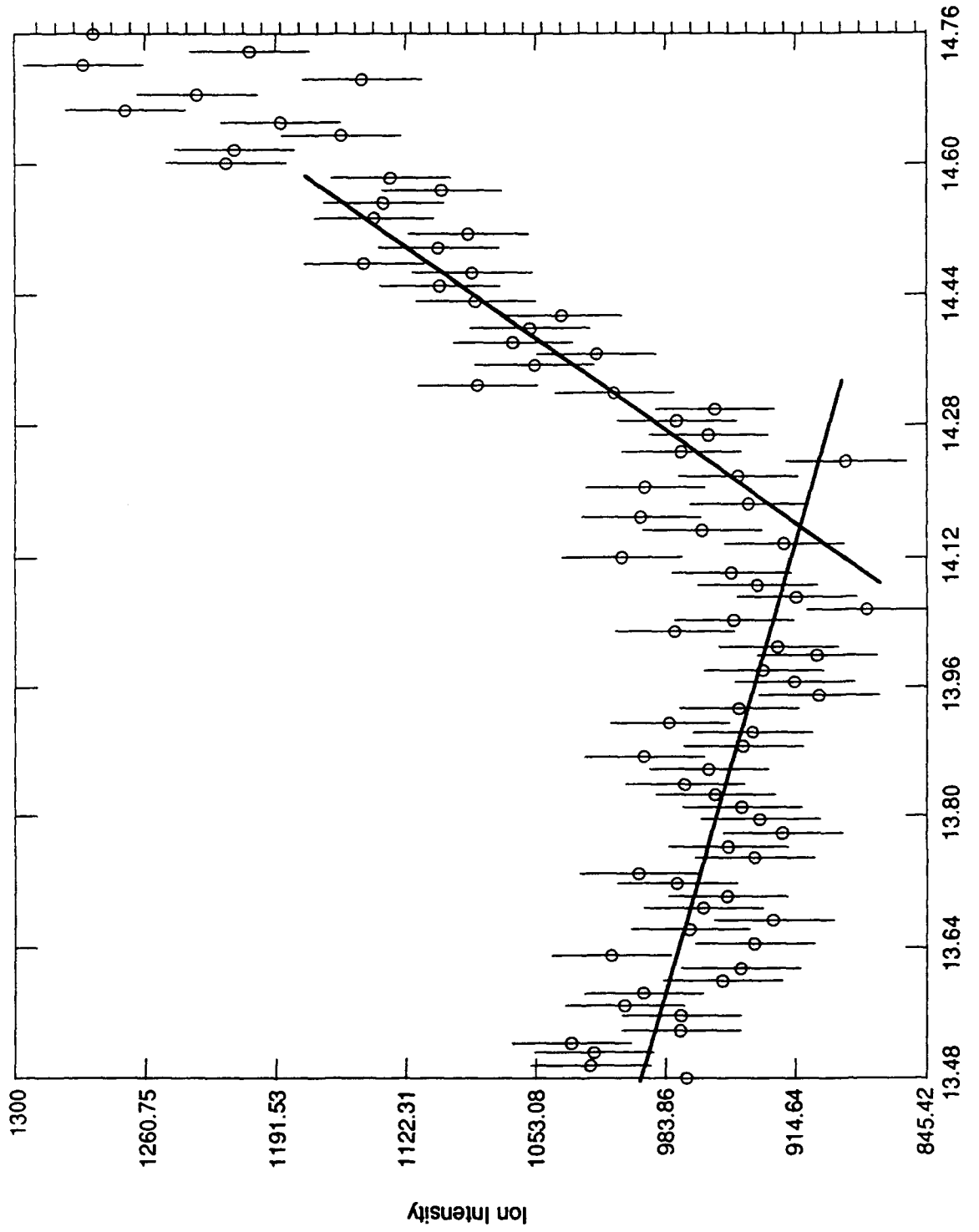

Figure 11. Onset Region for the Reaction $(C_6H_6 + O_2)_{trimers} + h\upsilon \rightarrow C_6H_6O^+ + Other\ Products.$

If benzene is assumed to be the chromophore for this process, it is very interesting that the excitation energy of the benzene ion is 114 ± 2 kcal mol^{-1}, very close to the dissociation energy of isolated O_2 at 118 kcal mol^{-1}. One can envision a mechanism in which the energy in the excited benzene ion transfers to a highly excited vibronic state of the O_2, followed by its dissociation. Appropriate states could be the $c'\Sigma_u$, $C^3\Delta_u$, or $A^3\Sigma_u$, all of which are reasonable because they are stretched with respect to the ground state. One oxygen atom escapes while the other is captured by the $C_6H_6^+$ ion. Measurement of the distribution of product translation energies using an ion kinetic energy lens described later would help confirm or contradict the above and other proposed mechanisms.

Measurements have also been made for C_6F_6 + O_2, but analysis of this is needed. The dissociation energy of $C_6F_6 \cdot O_2$ is significantly larger than that of $C_6H_6 \cdot O_2$, and once again a clear autoionization structure is observed just above its ionization potential (IP). A photoionization-induced dissociative rearrangement to produce $C_6F_6O^+$ occurs with energetics similar to those described above for the production of $C_6H_6O^+$; however, further work would be needed to determine whether it is produced from heterodimers.

The behavior of both oxygen-containing complexes, $C_6H_6 \cdot O_2$ and $C_6F_6 \cdot O_2$, is typical of experiences with dissociative photoionization in other complexes. That is, products resulting from dissociation of the strong bond in O_2 were clearly identified in both cases. Products from the dissociation of O_2 are formed even though the O_2 is very weakly bound to either $C_6H_6 \cdot O_2$ or $C_6F_6 \cdot O_2$ in the complex. The yield of $C_6H_6O^+$ increases significantly if two C_6H_6 molecules are in the complex.

B. O_2 PLUS CF_3Br

To provide a context in which to understand the following experimental results, note that three systems were studied: (a) a fuel (C_6H_6 or C_6F_6) plus O_2 and (b) Halon 1301 (CF_3Br) plus O_2. The first two systems were described in Section IV.A. The results of the study of the O_2 + CF_3Br system are presented here. Weakly bound molecular complexes of all of these pairs were produced in supersonic-nozzle expansions.

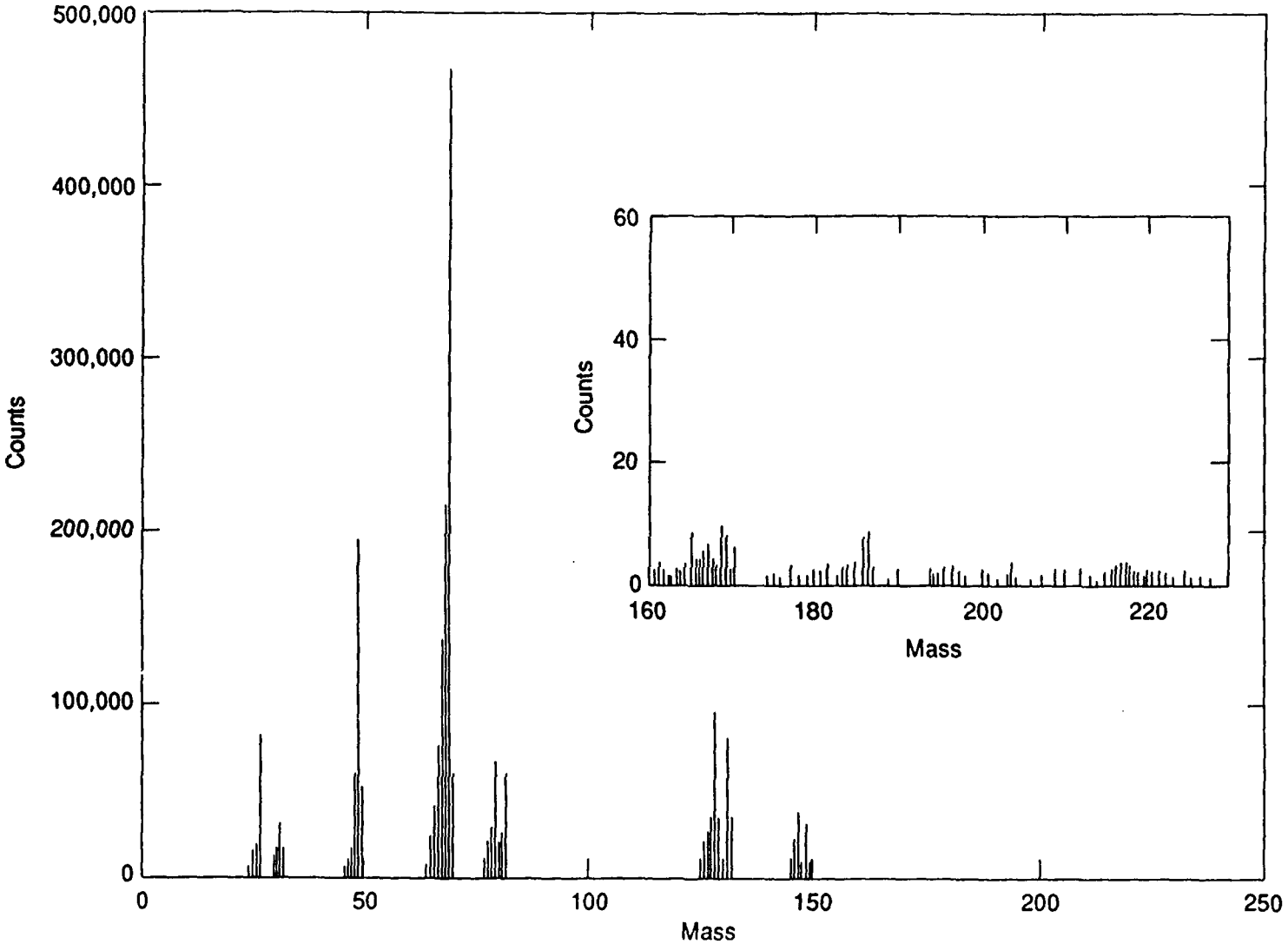

Figure 12. Mass Spectrum of CF_3Br at 584 Å (21.22 eV) Taken at a Nozzle Pressure of 97 Torr. (The inset shows an expanded scale of the m/e = 160 to 230 region.)

and their dissociation energies were determined. The results are given in Table 2. The dissociation energies are all small, 2 kcal mol^{-1} or less, confirming the weak binding. In the case of CF_3Br, the complex with oxygen could be formed in low concentration, but the homoclusters, $(CFBr)_n$, $n > 1$, were present in surprising abundance. Interference from these clusters was minimized by the use of very dilute mixtures (195:5) of CF_3Br in O_2 and maintenance of low nozzle stagnation pressures.

TABLE 2. DISSOCIATION ENERGIES OF THE WEAK MOLECULAR COMPLEXES $C_6H_6 \cdot O_2$, $C_6F_6 \cdot O_2$, $CF_3Br \cdot O_2$, AND THEIR IONS.

Mixture	Composition	Species	D°_o, kcal/mol^{-1}	D°_{298}, kcal/mol^{-1}
$C_6H_6 + O_2$	99.7:0.3	$C_6H_6 \cdot O_2$	1.20 ± 0.45	0.5 ± 0.5
		$C_6H_6 \cdot O_2^+$	2.86 ± 0.48	
$C_6F_6 + O_2$	99.7:0.3	$C_6F_6 \cdot O_2$	2.2 ± 0.5	
		$C_6F_6 \cdot O_2^+$	[a]3.3	
$CF_3Br + O_2$	95:5	$CF_3Br \cdot O_2$	[a]<2	
		$CF_3Br \cdot O_2^+$	[a]>3	

[a]Unrefined results.

In the cases of both $C_6H_6 \cdot O_2$ and $C_6F_6 \cdot O_2$, oxygenated fragments ($C_6H_6O^+$ and $C_6F_6O^+$) could be readily observed with the mass spectrometer. An attempt was made to prepare oxygenated fragments of $CF_3Br \cdot O_2$ by dissociative photoionization. The mass spectrum of neat CF_3Br in a molecular beam with a nozzle pressure of 97 torr was taken using 700 Å ionizing radiation (Figure 12). The fragmentation pattern is straightforward with very little parent ion CF_3Br^+ appearing at m/e = 148, 150, and fragments as follows: CF_2Br^+ (m/e = 129, 131); Br^+ (m/e = 79, 81); CF_3^+ (m/e = 69); CF_2^+ (m/e = 50). The dominant peak is due to CF_3^+. Careful examination of the m/e = 160

to 230 portion of the mass spectrum shows low background in this mass range. In particular, a signal appears in the vicinity of m/e = 166 to 171, but virtually none at m/e = 180, 182, where $CF_3Br{\bullet}O_2^+$ peaks should appear.

The weak complex $CF_3Br{\bullet}O_2$ was prepared by expanding a 1:20 mixture of CF_3Br in O_2 through the nozzle at a pressure of 1741 torr and cooling the nozzle to 1 °C. The mass spectrum obtained using 700 Å light is shown in Figure 13. Only the higher mass region, m/e = 110 to 250, is shown in this figure. Note the two sets of peaks resulting from ionization of the monomer (CF_3Br^+) and m/e = 129, 131 (CF_2Br^+), respectively. The latter fragment comes from a $(CF_3Br)_2$ or larger cluster, which forms in appreciable abundance even in this dilute mixture. Although the amount of $CF_3Br{\bullet}O_2$ is small, the signal is sufficient to determine the ionization potential of the complex.

Photoion yield curves through the ionization threshold region were run for both CF_3Br and $CF_3Br{\bullet}O_2$ (Figures 14 through 16). The curve in Figure 14 has been analyzed to give an ionization threshold of CF_3Br at 1078 Å, which corresponds to an ionization potential of 11.50 eV. The dissociation energy of the F_3C-Br bond is known to be 3.78 eV = 87.2 kcal mol^{-1}. This value is typical of carbon-bromine bond strengths in organic molecules.

The photoion yield curves in Figures 15 and 16 have been analyzed to give an ionization potential for the formation of $CF_3Br{\bullet}O_2^+$ from $CF_3Br{\bullet}O_2$ of 1083 Å = 11.45 eV. The decrease in ionization potential is typical of many observations of cluster formation; however, it is much smaller than customarily noticed. It is not uncommon to observe ionization potential decreases of 0.5 to 0.7 eV, in contrast to the change of 0.05 eV seen here. This dramatic observation suggests unusual bonding properties in the $CF_3Br{\bullet}O_2^+$ cation. Combining the ionization potentials of CF_3Br and $CF_3Br{\bullet}O_2$ with the measured dissociation energy of the weak complex $CF_3Br{\bullet}O_2$, allows an estimate of approximately 3 kcal/mol^{-1} for the bond dissociation energy in the ion, $CF_3^+Br{\bullet}O_2$, (Table 2). This bond strength is very similar to cation bond strengths in

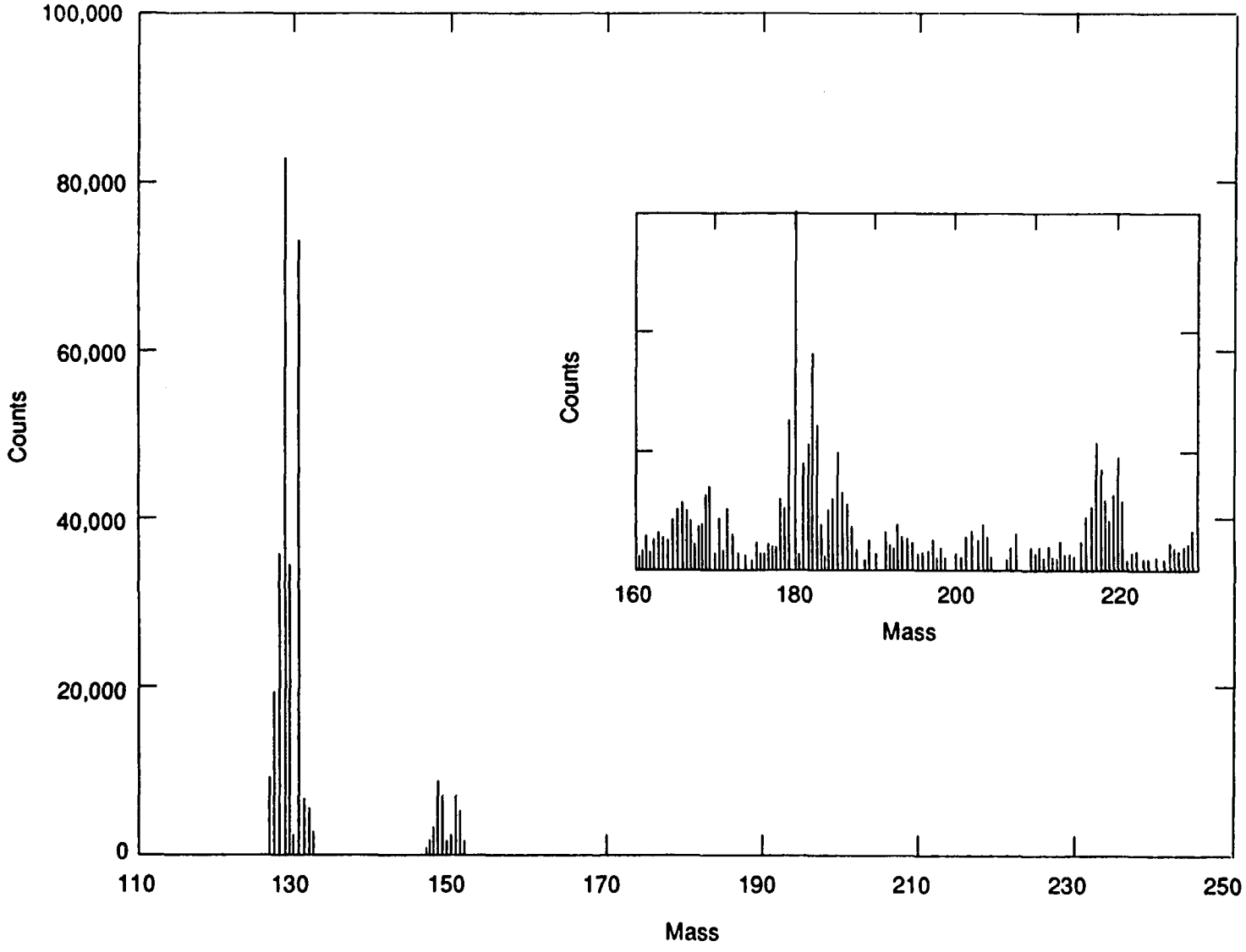

Figure 13. Mass Spectrum of a 1:20 Mixture of CF_3Br in O_2 at 700 Å (17.71 eV). (The nozzle stagnation pressure was 1741 torr and the mass range displayed is m/e = 110 to 250. The inset gives the expanded scale portion over the mass range of m/e = 160 to 230.)

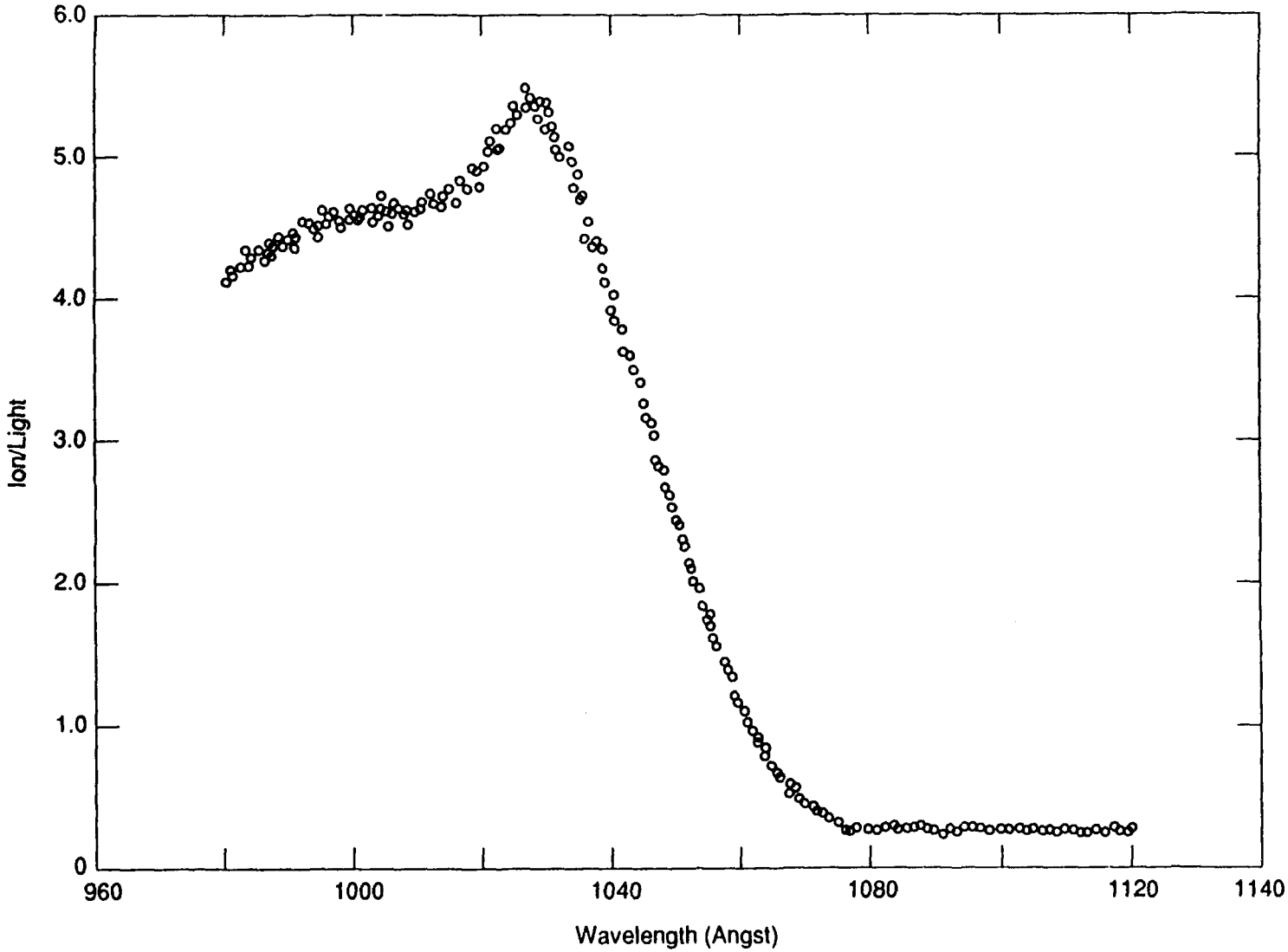

Figure 14. CF_3Br^+ Photoion Yield Curve Over the Range 980 to 1120 Å. (The observed intensities of the ion CF_3Br^+ produced direct ionization of neat CF_3Br at 499 torr nozzle pressure in 0.5-Å intervals. No LiF filter was used and corrections for second-order contributions have not been applied. The threshold is IP (CF_3Br^+) = 11.50 ± 0.02 eV (1078 Å).)

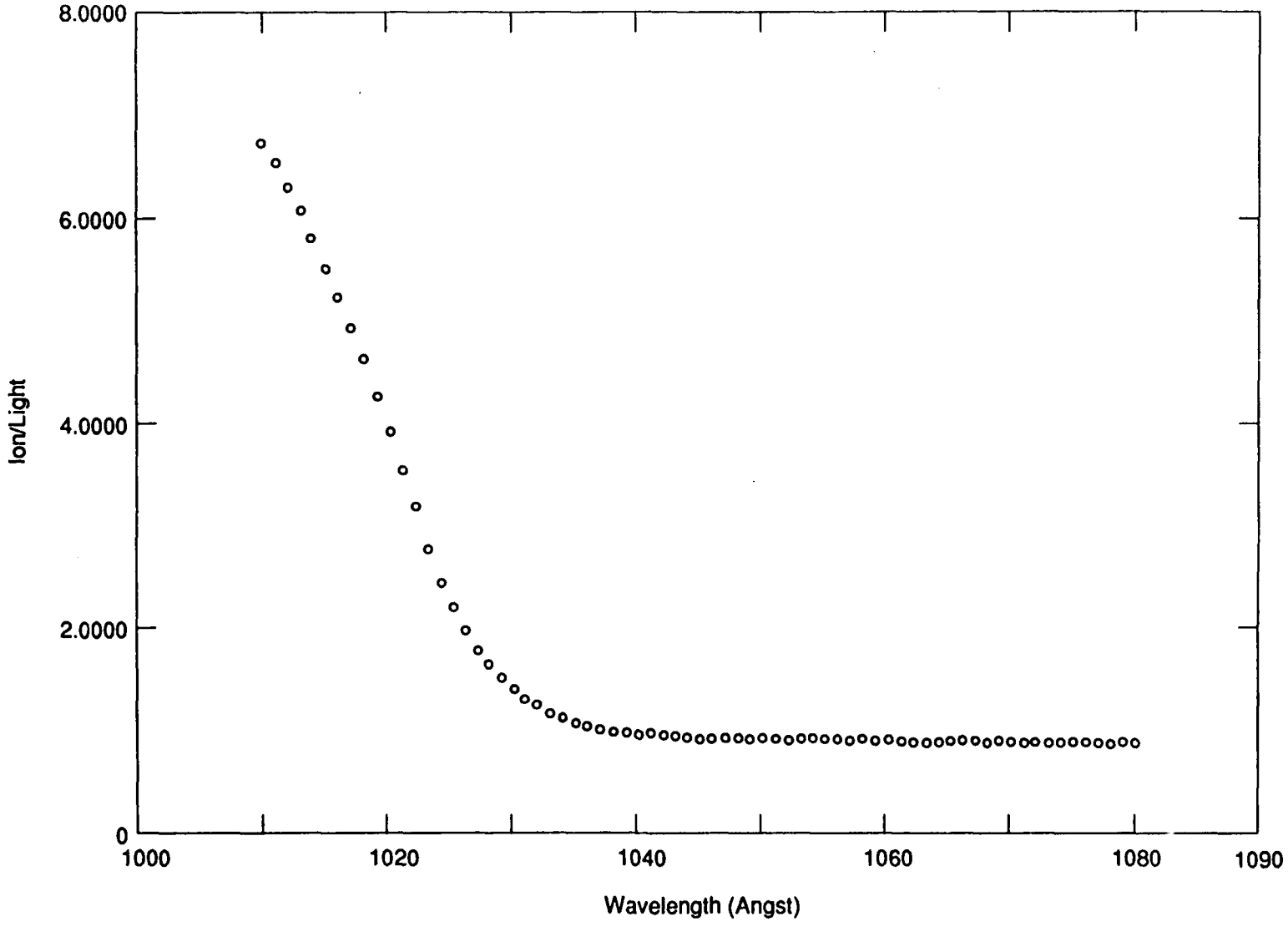

Figure 15. CF_3^+ Photoion Yield Curve Over the Range 1010 to 1080 Å. (Observed intensities of the ion CF_3^+ produced by direct ionization of CF_3Br in a 1:20 mixture of $CF_3Br + O_2$ at 604-torr nozzle pressure in 1 Å intervals. No LiF filter was used. The nozzle temperature was 1.1° C. The threshold is $AP(CF_3^+) = 12.0 \pm 0.1$ eV (1033 Å).)

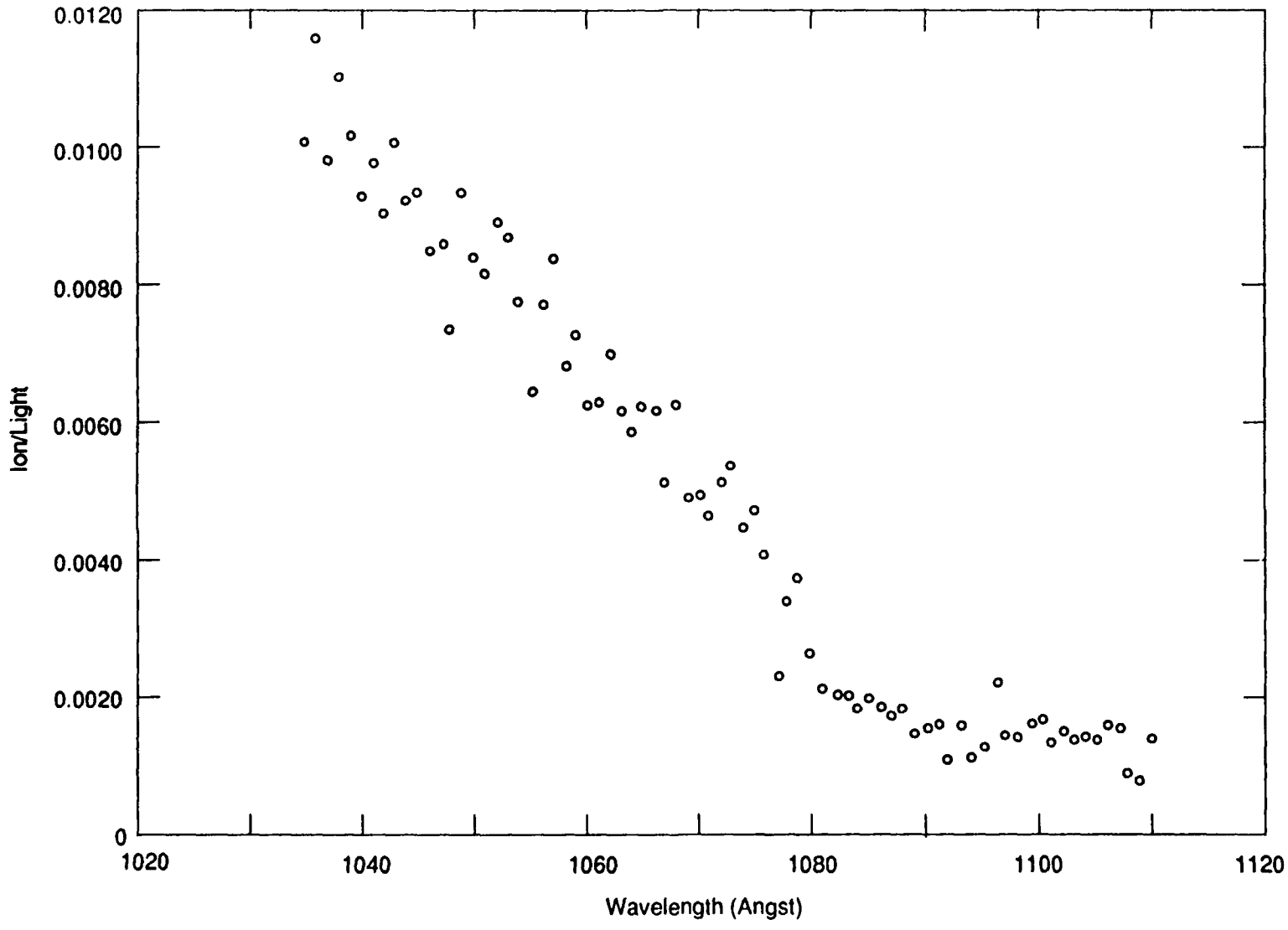

Figure 16. Photoion Yield Curve for $CF_3BrO_2^+$ Over the Range 1035 to 1110 Å. (Threshold photoion yield curves for the production of CF_3BrO_2 from $CF_3Br \cdot O_2$ with a nozzle pressure of 1:20 CF_3Br+O_2 at 1750 torr and with no LiF window. Second-order corrections have not been applied. The intervals were 1 Å, and the total counting time at each wavelength was 70 sec. The results give $IP(CF_3Br \cdot O_2) = 11.45 \pm 0.04$ eV (1083 Å).)

$C_6H_6 \cdot O_2$ and $C_6F_6 \cdot O_2^+$. The result suggests that one or more of the bonds in CF_3Br^+ are unusual. Therefore, the appearance potential of CF_3^+ from CF_3Br was measured by dissociative photoionization of a molecular beam of $CF_3Br + O_2$. The results are shown in Figure 15.

By applying second-order corrections to the curve in Figure 15, an appearance potential of 1033 Å = 12.0 eV for CF_3^+ from CF_3Br has been determined. This result can be combined with the ionization potential of CF_3Br (11.50 eV) to give a bond strength of the C-Br bond in F_3C^+-Br of 0.5 eV = 12 kcal mol^{-1}. This is an extremely weak bond and cannot involve a chemical bond in the sense of electron sharing between CF_3^+ and Br. It is characteristic of an ion-induced dipole interaction between these two species. It appears that this weak bond is the basis for the very small shift in ionization potential in $CF_3Br \cdot O_2$.

The thermodynamic information for the species in the CF_3Br system is collected in the energy diagram shown in Figure 17.

A careful search of the mass spectrum for oxygenated fragments of $CF_3Br \cdot O_2$ prepared by dissociative photoionization was conducted. It was discussed earlier that oxygenated fragments were observed in the $C_6H_6 \cdot O_2$ and $C_6F_6 \cdot O_2$ systems. Figure 18 shows the mass spectra for the regions in which CF_3O^+ (m/e = 85), CF_2BrO^+ (m/e = 145, 147), and CF_3BrO^+ (m/e = 164, 166) would be expected to appear; however, no distinct peaks can be observed in the m/e = 83 to 87 or 143 to 149 regions. The signal here is background only. Note that the characteristic set of two peaks corresponding to the bromine isotopes is completely absent in the m/e = 143 to 149 segment. The situation is somewhat less clear at m/e = 145, 147 because this region is located in the low mass wing of the CF_3Br^+ parent ion at m/e = 148, 150. Nevertheless, no feature resembling the doublet expected for the two bromine isotopes appears at the appropriate masses. Although this study was repeated several times at different compositions and nozzle pressures, no oxygenated fragments of $CF_3Br \cdot O_2$ dissociative photoionization were detected.

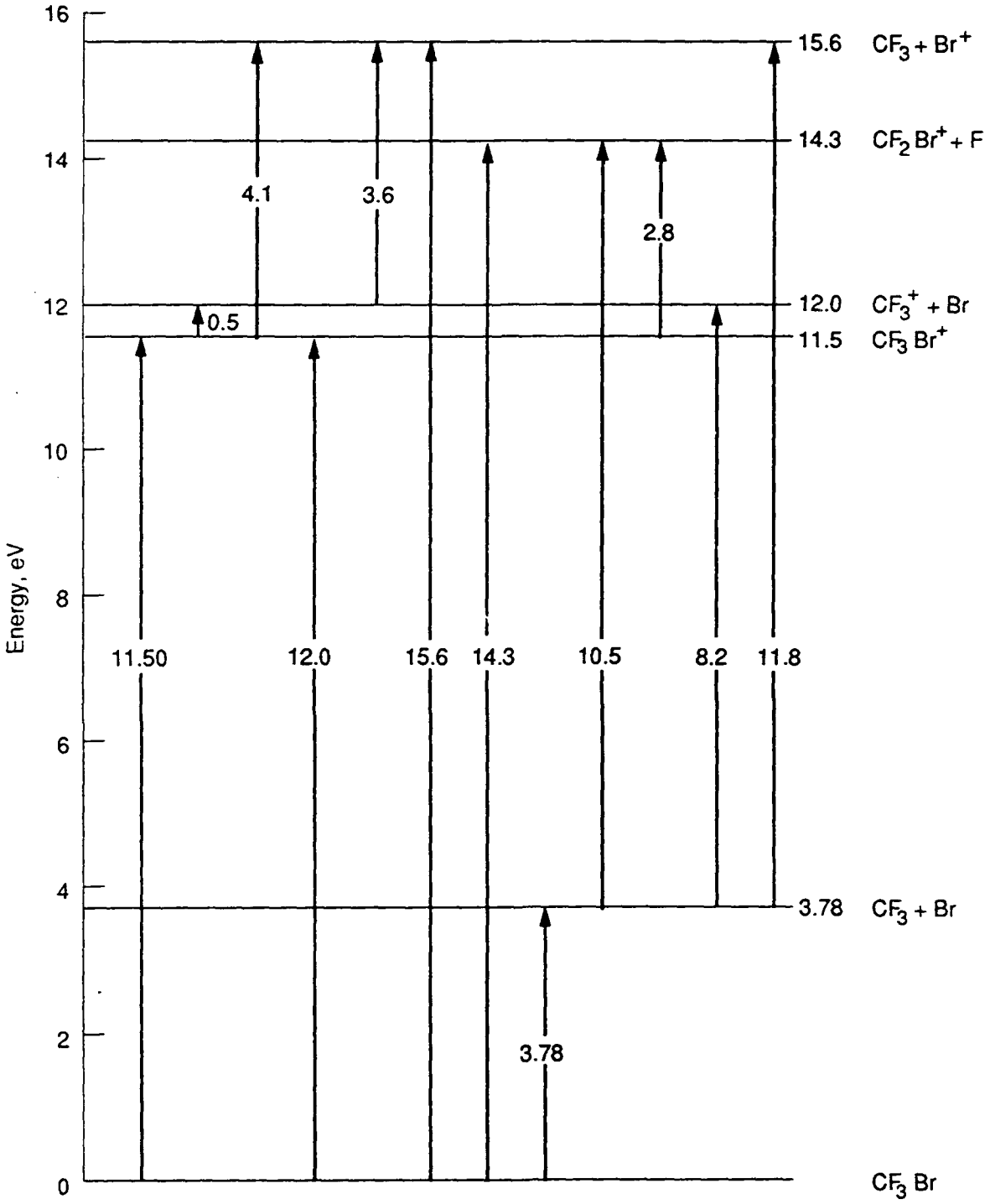

Figure 17. Energy Diagram for the Neutral and Ionic Species in the CF_3Br System.

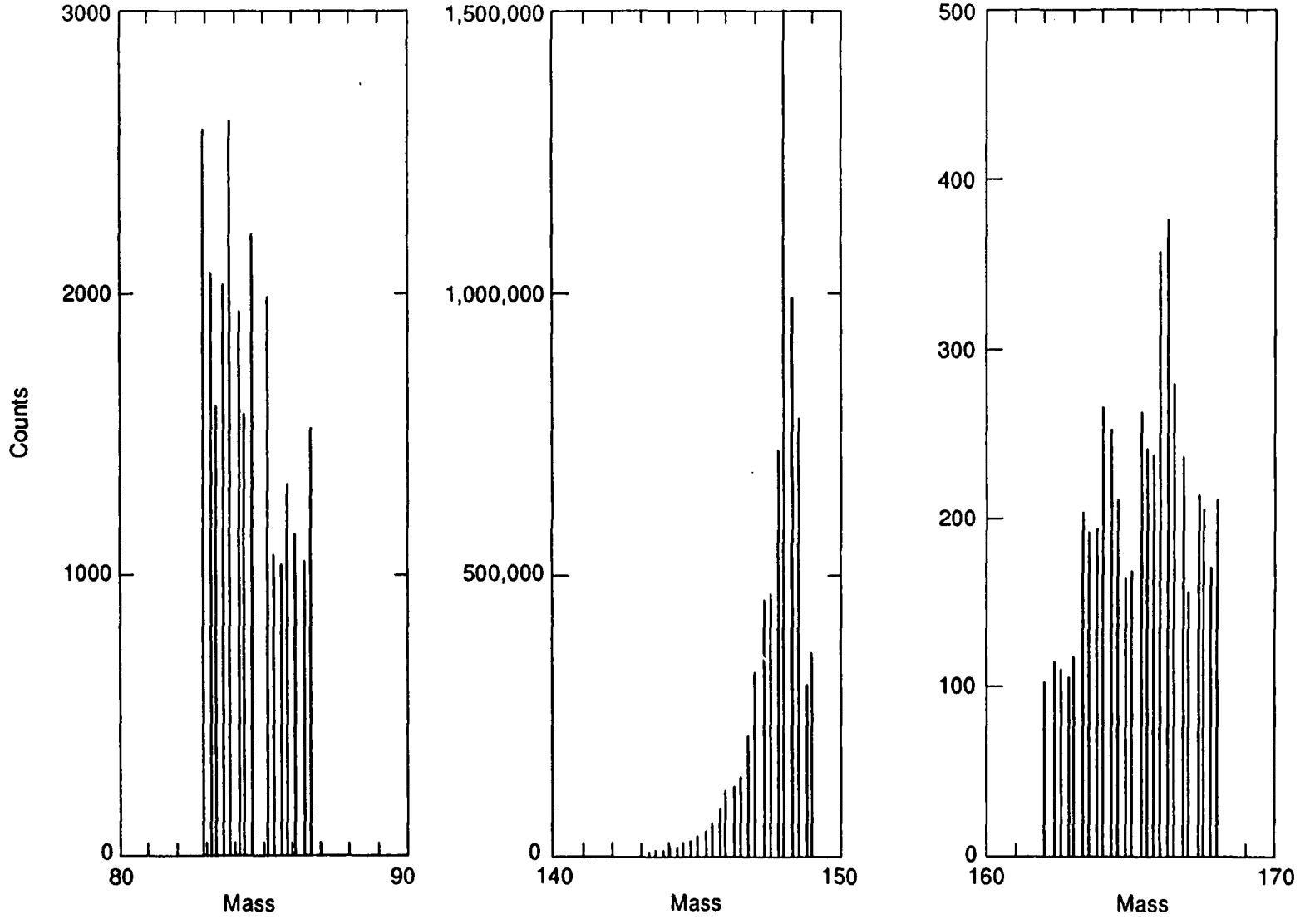

Figure 18. Detailed Mass Spectra of 1:20 $CF_3Br:O_2$ at 700 Å with a Nozzle Pressure of 1750 Torr. (The ranges covered are m/e = 83 to 87, 143 to 149, and 162 to 168 in 0.25-amu steps. The counting time at each mass setting was 40 sec.)

Quantum mechanical calculations on the CF_3Br^+ system were carried out using the AM1 suite of programs. This semiempirical approach has been optimized to give good heats of formation for both neutrals and ions. The small C-Br bond energy in the cation (12 kcal mol^{-1}) was confirmed by the calculation. By stretching the C-Br bond and allowing the incipient CF_3^+ to relax, a shallow well was produced with a minimum at a long C-Br distance of approximately 3.30Å. The charge distribution suggests that the species is an ion-induced dipole complex between CF_3^+ and Br. The calculated enthalpy as a function of C-Br bond length is shown in Figure 19 for the neutral molecule CF_3Br. The same information for the ion CF_3Br^+ is given in Figure 20. From these figures it is clear that CF_3Br^+ is much more weakly and loosely bound than CF_3Br.

In summary, the weakly bound molecular complex between Halon 1301 (CF_3Br) and O_2 has been studied by photoionization mass spectrometry in a molecular beam. Ionization and appearance potentials for many of the species in this binary system have been determined. The most striking result is the inability to detect oxygenated fragments of dissociative photoionization of the complex $CF_3Br \cdot O_2$. This is doubtless because of the fragility of CF_3Br^+, for which the CF_3^+-Br bond strength was measured to be only 12 kcal mol^{-1}. These extraordinary results yield a number of implications for the role of CF_3Br in fire extinguishment.

(1) A reevaluation of the canonical mechanism for interaction of CF_3Br with flame free radicals may be necessary. The results suggest that CF_3Br may not directly serve as a trap for the O-atoms in a flame. Perhaps a supplementary oxygen atom trapping agent could be found to enhance the fire extinguishment properties of a halon or halon replacement.

(2) The extremely weak C-Br bond in CF_3Br^+ suggests that Br atoms can enter the flame via the ion CF_3Br^+ and not only from CF_3Br itself. If this is substantiated, the door to many possible alternative agents is opened.

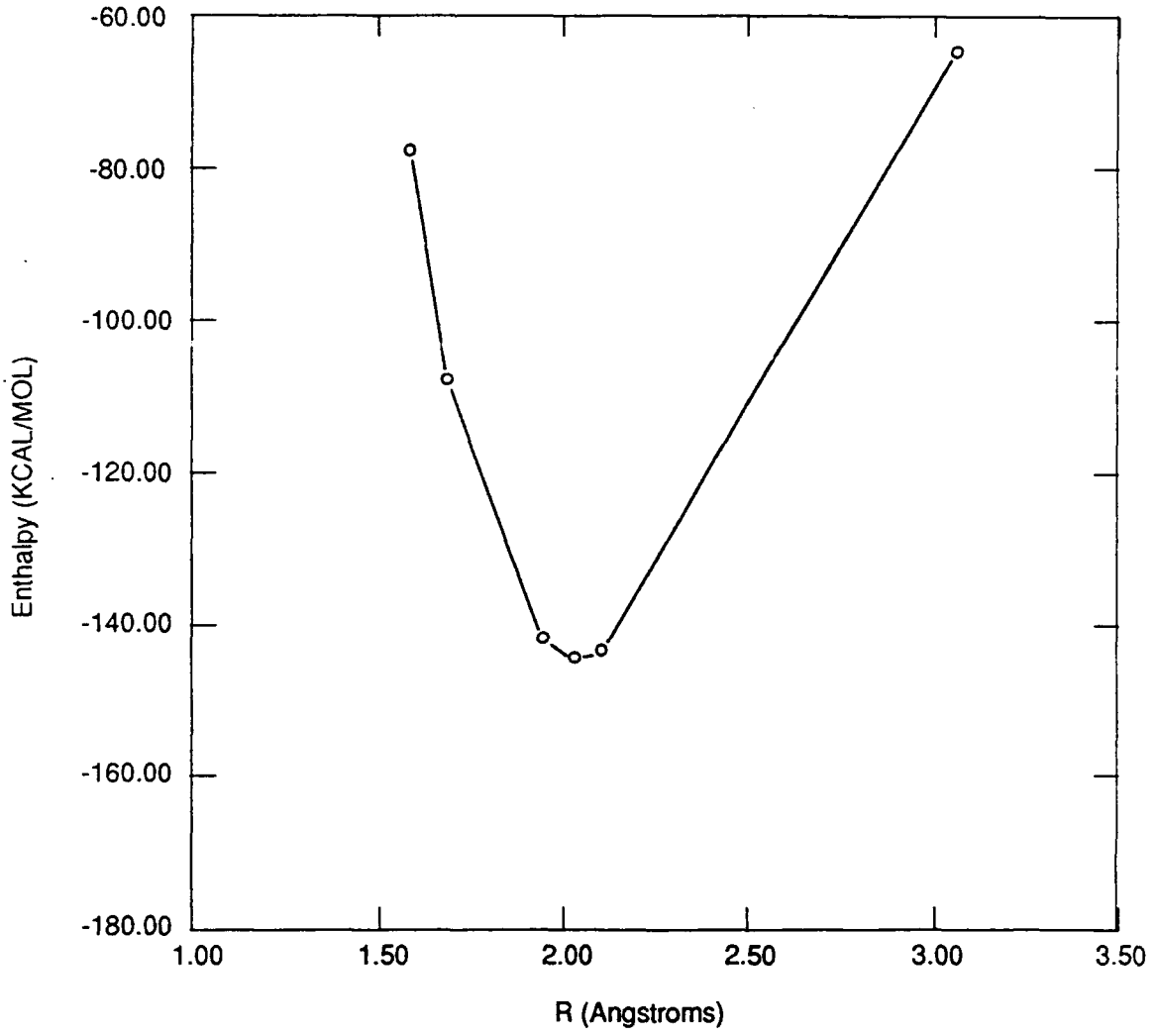

Figure 19. Enthalpy versus CF_3-Br Bond Distance.

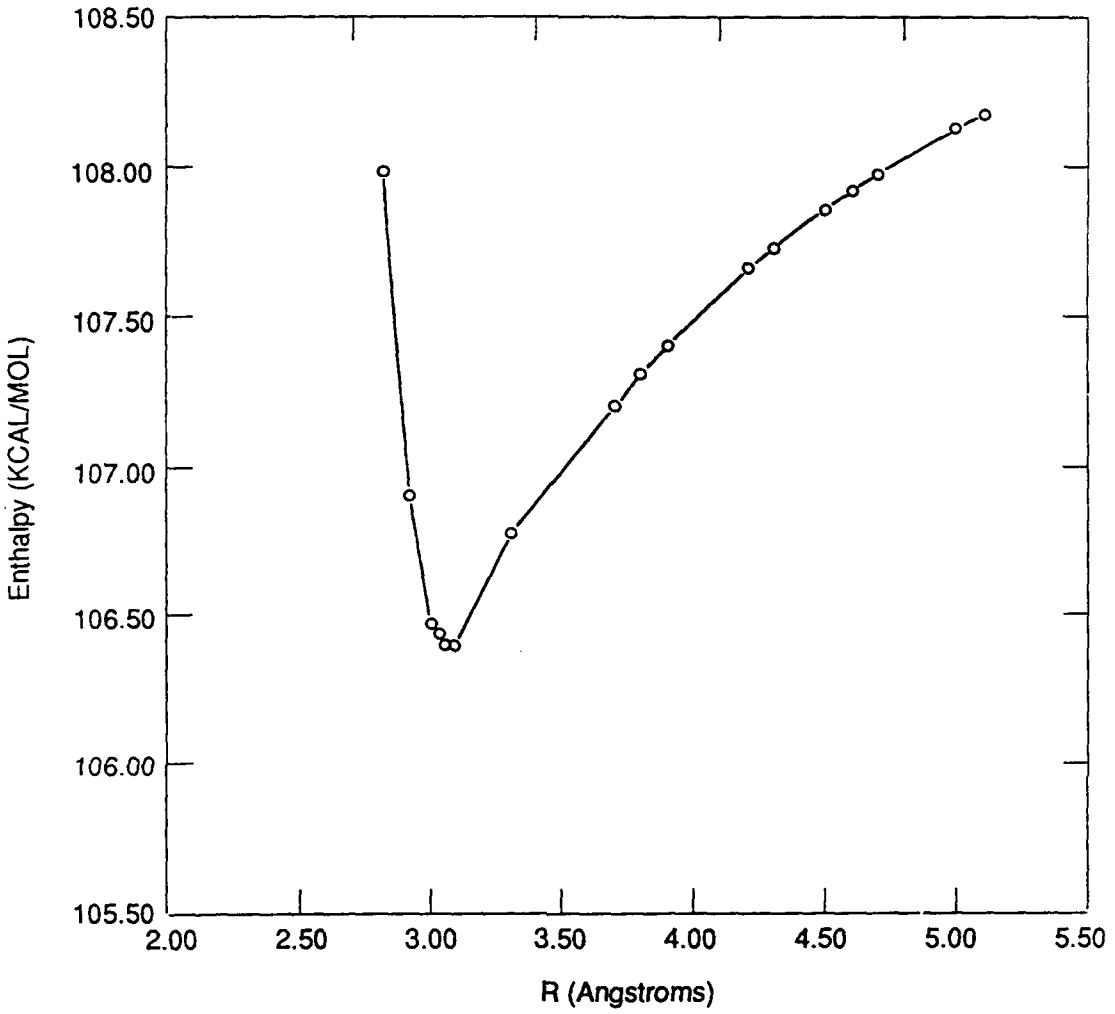

Figure 20. Enthalpy versus CF_3^+- Br Bond Distance.

(3) The role of the CF_3 portion of the halon may be more significant than previously suspected. It may not simply be a spectator in the process of free-radical-trapping agent release, but a chemically active participant in trapping free radicals.

(4) If the Br in the halon molecule does trap flame free radicals directly, the radicals trapped must be H or OH. The evidence presented here shows that Br in the CF_3Br molecule does not react well with O.

C. CF_3Br PLUS CH_3OH

Some complexes of polyatomic molecules are difficult to synthesize in expansions of binary mixtures, notably the heteroclusters of CF_3Br and CH_3OH. Nevertheless, it is important (1) to be able to make any complex at will, for example, to study any nonbonding interactions that may be of interest, and (2) to investigate photoinduced intracluster reactions between an arbitrary pair of weakly associated reactant molecules. For the synthesis of recalcitrant clusters in nozzle expansions it is often useful to add a third component, such as a noble gas, to the gas mixture to increase the cooling ability of the jet at a given nozzle pressure. For the first time, a study of the products of free-jet expansions, which has been previously restricted to binary mixtures, has been extended to ternary mixtures.

In general, understanding expansions well enough to be able to predict conditions to optimize the cluster of interest is a goal that has not yet been reached. As noted with regard to some earlier work, experimental results may be compromised when it is not known which expansion products are dominant (Reference 9). Consequently, careful experimental determination of neutral cluster distributions in molecular beams is essential.

Bromotrifluoromethane clustering in jet expansions has not been studied until recently, despite the outstanding flame-suppression abilities of this compound. On the

other hand, clusters of methanol have been studied extensively, although the jet condensation behavior of methanol has been mentioned only infrequently, for either homogeneous (References 10 through 16) or mixed clusters (References 17 through 20). Three papers report cluster distributions determined by electron impact ionization-mass spectrometry with the concomitant loss of some information resulting from the unknown influence of fragmentation (References 15, 19, and 20). In another experiment, cluster sorting via angle-discriminative scattering in crossed beams was exploited to optimize conditions for the production of methanol dimers and trimers in expansions of methanol seeded in helium and neon (Reference 9).

These results of this study extend to ternary gas mixtures, while a study of the products of free-jet expansions was previously restricted to binary mixtures. As discussed above, some complexes of polyatomic molecules (for example, the heteroclusters of CF_3Br plus CH_3OH) are difficult to synthesize in expansions of binary mixtures because of slow cooling. To overcome this problem, it is useful to add a third component to the gas mixture, such as a noble gas, to speed the cooling rate of the jet at a given nozzle pressure. Therefore, to find an efficient way to prepare $CH_3OH{\bullet}CF_3Br$ and the corresponding larger mixed complexes, the distribution of neutral clusters formed in free-jet expansions of CH_3OH + CF_3Br + Ar was investigated. For analysis of the expansion products, the method of near-threshold one-photon photoionization was used (Reference 3). Results are shown in Figures 21 and 22.

Figure 21 shows the nozzle pressure dependences of the beam number densities of the clusters $(CF_3Br)_2$, $(CH_3OH)_2$, $(CH_3OH)_3$, $CF_3Br{\bullet}CH_3OH$, and $CF_3Br(CH_3OH)_2$. Smooth curves drawn through the points were used to represent the data in the calculations of relative proportions. The curves of Figure 21 are assembled in their approximate relationship in Figure 22. The curve for $(CH_3OH)_3$ is somewhat too high because the contributions of $(CH_3OH)_3$ and $CF_3Br{\bullet}CH_3OH$ cannot be resolved with the present data. This high curvature is a consequence of the resolution method, which involves the solution of simultaneous equations, and thus requires distinctly different behavior of the number density curves in the region used for the analysis. However, the relative intensities of the ions $(CF_3Br{\bullet}CH_3OH)^+$ and $(CH_3OH)_3^+$ suggest that the

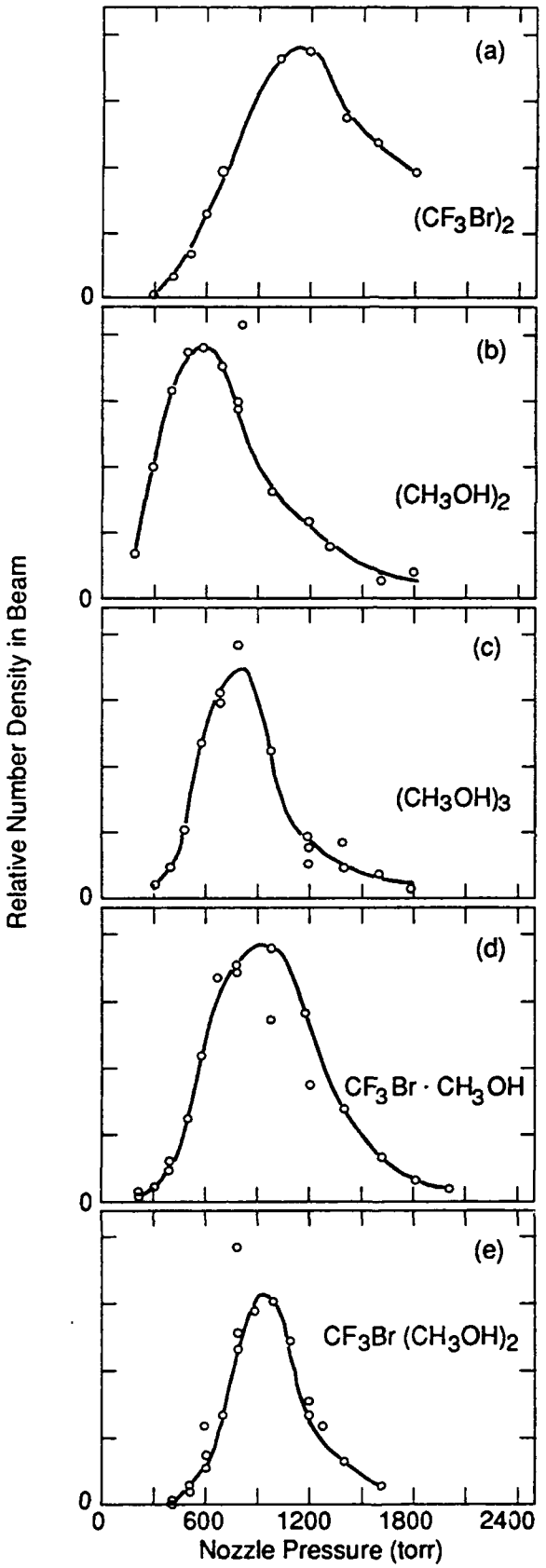

Figure 21. Nozzle Pressure Dependences of the Beam Number Densities of the Clusters $(CF_3Br)_2$, $(CH_3OH)_2$, $(CH_3OH)_3$, $CF_3Br{\bullet}CH_3OH$, and $CF_3Br(CH_3OH)_2$ Formed in the Free-jet Expansion of the Ternary Mixture CH_3OH + 28 CF_3Br + 293 Ar.

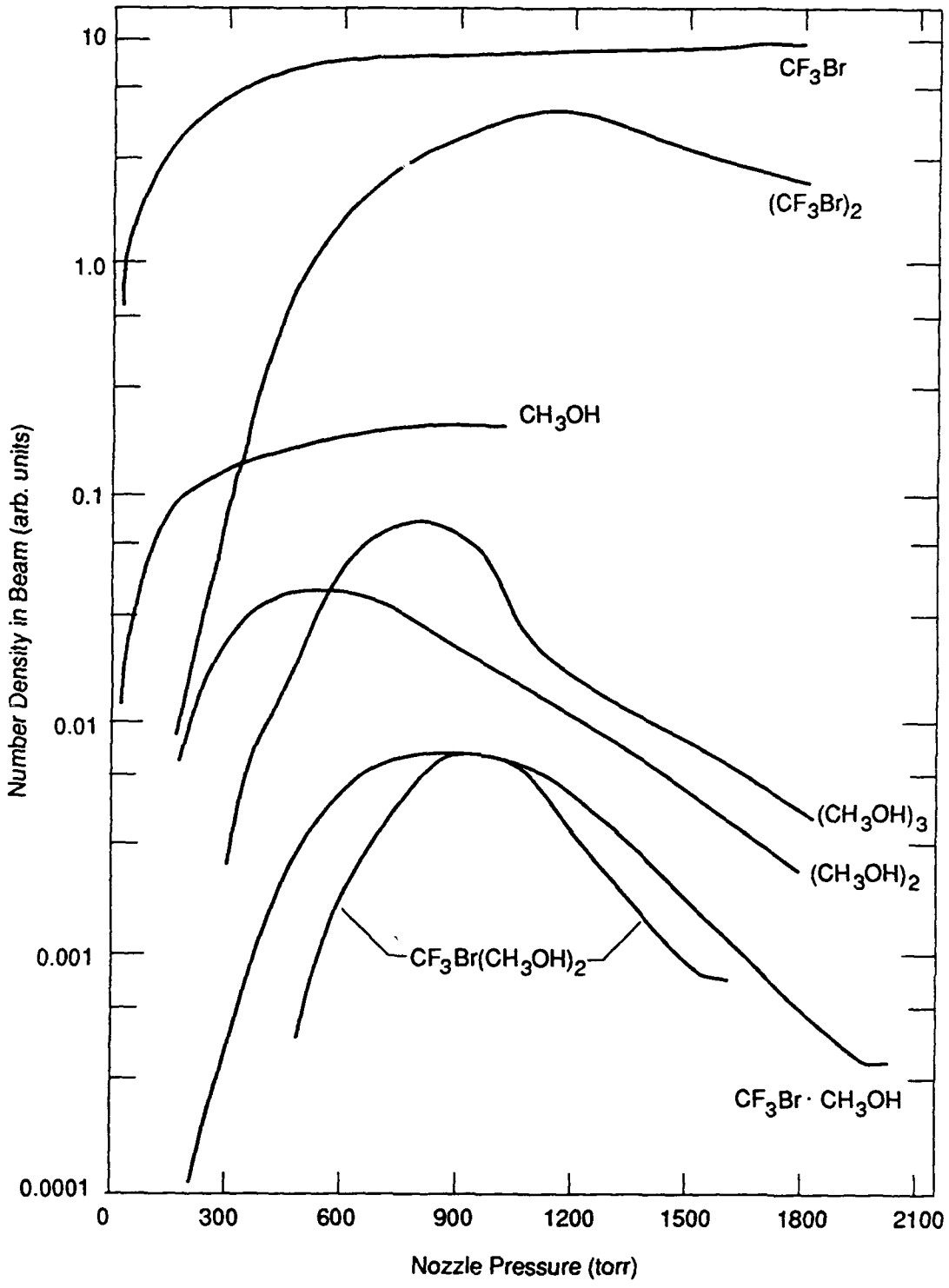

Figure 22. Summary of Relative Number Densities of Neutral Clusters Formed in the Free-jet Expansion of the Ternary Mixture $CH_3OH + 28CF_3Br + 293Ar$, Using a 0.010-cm Nozzle at Room Temperature.

neutral $(CH_3OH)_3$ is by far the more intense. Similarly, the relative heights of the curves for $CH_3Br{\bullet}CH_3OH$ and $CF_3Br(CH_3OH)_2$ cannot be ascertained, although the corresponding ion yields indicate that they may be roughly comparable. The latter curves have therefore been arbitrarily plotted with the same maximum heights, and positioned about an order of magnitude lower than the curve for $(CH_3OH)_3$, consistent with the above considerations.

The curves for the dimers $(CH_3OH)_2$ rise at lower nozzle pressures than the trimers $(CH_3OH)_3$, as expected for a competitive mechanism. Parallel behavior occurs for the heteroclusters $CF_3Br{\bullet}CH_3OH$ and $CF_3Br(CH_3OH)_2$. However, $(CH_3OH)_2$ rises at lower pressure than $CF_3Br{\bullet}CH_3OH$, which may indicate a larger dissociation energy for $(CH_3OH)_2$ than for $CF_3Br{\bullet}CH_3OH$. The relative rate of increase of $(CF_3Br)_2$ exceeds only that of $CF_3Br(CH_3OH)_2$, and the pressure of its maximum, 1150 torr, is the highest of all. This high-pressure maximum suggests that the dissociation energy of $(CF_3Br)_2$ may be the smallest of the three dimers.

All of the curves, except that of $(CF_3Br)_2$, fell rapidly as the nozzle pressure increased beyond the maximum of each. This behavior contrasts sharply with that observed in several other expansions (References 8 and 21), in which the number densities fall only slowly, but it is similar to the rapid decreases noted in clusters of noble gases seeded with tetracene (Reference 22). Since such contrasting behavior is not to be expected of a simple equilibrium model (Reference 16), it substantiates the dominance here of dynamical processes in determining the distribution of products of the jet expansions.

The disposal of total CF_3Br and CH_3OH into clusters is shown in Figures 23 and 24. As stated before, the curve for $(CH_3OH)_3$ shown in Figure 24 is somewhat overestimated. The correction to the curve for $(CF_3Br)_2$ for $CF_3Br{\bullet}CH_3OH$ and $CF_3Br(CH_3OH)_2$ is negligible. Note that even at the mixing ratio $CH_3OH{:}CF_3Br$ = 1:28, CH_3OH clusters much more readily than CF_3Br does.

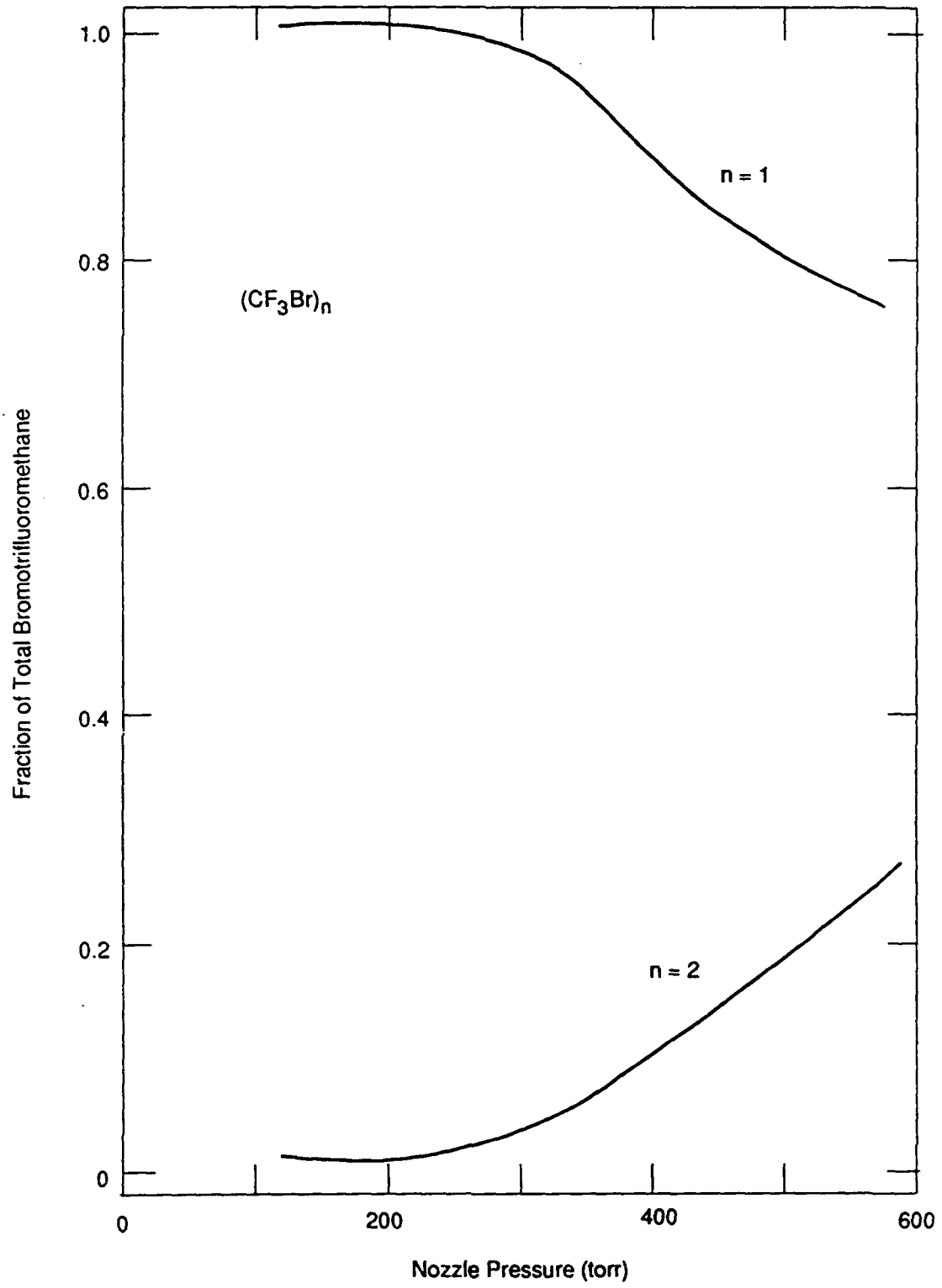

Figure 23. Formation of Clusters of Halon 1301 Molecules as a Function of Pressure.

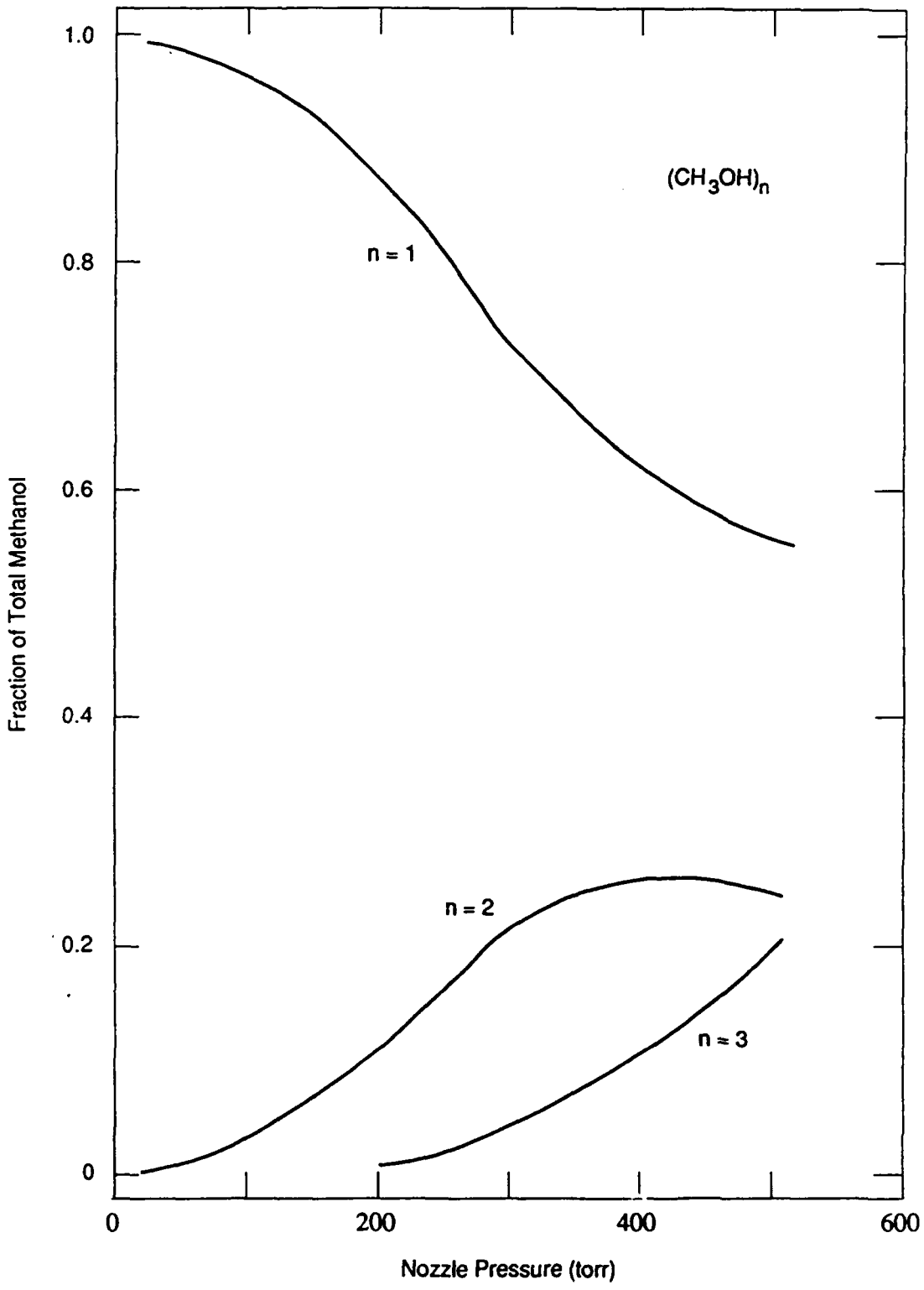

Figure 24. Formation of Clusters of Methanol Molecules as a Function of Pressure.

Table 3 compares the known data in which the number density distribution of dimers versus nozzle pressure has been measured. The value given for $P_{1/2}$ represents the pressure at which the number density has reached half its maximum value on the low pressure side. The pattern is about what is expected if the clusters are formed in regions of the expansion in which continuum (equilibrium) effects dominate. These data reflect the well-known fact that different degrees of freedom cool at different rates so the extent of cluster formation as a function of nozzle pressure depends strongly on dynamical processes occurring in the expansion (Reference 21). It is interesting to note, however, that whenever more than one dimer is formed in the same expansion. The dimer with the largest dissociation energy rises at the lowest pressures, and the dimer with the smallest dissociation energy rises at the highest pressures. The pressures for maximum abundance of the important dimers and trimers in this system are given in Table 4.

After conditions were established for the formation of dimers and trimers, dissociative photoionization phenomena were examined. Detailed mass spectra provided identification of the fragments of both monomeric species and clusters. The fragments of cluster dissociative photoionization are HBr^+, $(CH_3OH{\bullet}CH_3)^+$, $(CH_3OH{\bullet}Br)^+$, $(CH_3OH)_2Br^+$, and $(CH_3OH{\bullet}CF_3Br)Br^+$. All of the fragments arise from breakup of CF_3Br, with the appearance that CF_3Br acts as the chromophore resulting in $(CH_3OH)_nCF_3Br^+$ followed by the breakup of the very weak C-Br bond in the ion. Only the HBr^+ fragment supplies evidence of either H or OH radicals coming from the CH_3OH moiety. Specifically, neither $(CF_3Br{\bullet}OH)^+$ nor $BrOH^+$ was detected.

The significance of this observation is that the intracluster process appears to give the product corresponding to a reaction between Br and the H-atom flame free radical. No indication of reaction between Br and OH was found, which substantiates the earlier bulk results that CF_3Br initially quenches flames by trapping H atoms in HBr.

The appearance potentials of a number of cluster ions and fragments were measured. The results of these measurements are somewhat unrefined because the software for doing second-order corrections and summing spectra had to be written and

TABLE 3. COMPARISON OF CONDITIONS FOR PRODUCTION OF VARIOUS DIMERS.

Complex	Gas Mixture	$P_{1/2}$, torr	T_b, K	D_o, kcal mol^{-1}	References
$(CF_3Br)_2$	$CH_3OH:CF_3Br:Ar$ 1:28:293	700	5		
$CF_3Br•CH_3OH$	$CH_3OH:CF_3Br:Ar$ 1:28:293	560	6		
$(CH_3OH)_2$	$CH_3OH:CF_3Br:Ar$ 1:28:293	290	9	4.3 ± 0.5	
$C_2H_4•HCl$	$C_2H_4:HCl$ 1:4	260	21	3.2 ± 0.7	4, 24
$(1,3\text{-}C_4H_6)_2$	$1,3\text{-}C_4H_6:SO_2$ 1:9	460	50		25
$1,3\text{-}C_4H_6•SO_2$	$1,3\text{-}C_4H_6:SO_2$ 1:4	400	69	3.2 ± 0.5	25
$C_6H_5Cl•NH_3$	$C_6H_5Cl:NH_3$ 1:200	180	36	2.0 ± 0.3	8, 9
$(C_6H_6)_2$	$C_6H_6:Ar$ 1:9	150	16	2.4 ± 0.4	6, 26
$(C_6H_6)_2$	$C_6H_6:O_2$ 1:127	1100	7	2.4 ± 0.4	6, 26
$CH_6H_6•HCl$	$C_6H_6:HCl$ 1:9	150	35	4.8 ± 0.1	4, 27
$C_6H_6•O_2$	$C_6H_6:O_2$ 1:127	2100	5	1.2 ± 0.4	28

TABLE 4. NEUTRAL CLUSTERS AND NOZZLE PRESSURES OF MAXIMUM ABUNDANCE.

Neutral	Pressure, torr
$(CH_3OH)_2$	600
$(CH_3OH)_3$	810
$CF_3Br \cdot CH_3OH$	880
$CF_3Br(CH_3OH)_2$	1000
$(CF_3Br)_2$	1120

remains largely incomplete. Final data analysis may result in fairly small adjustments to the values in Figure 25.

D. CF_3Br PLUS METAL HYDRIDES

The ir spectrum of the vapors collected by condensing products of the reaction of CF_3Br with the hydride form of the alloy $LaNi_{4.7}Al_{0.3}$ displayed only the peaks belonging to CF_3Br plus a faint absorption due to HBr. This indicates reduction of CF_3Br at the metal hydride surface by atomic H in low yield. Reactions of this nature are known, but the extent of reaction is much less than anticipated. The most likely explanation is contamination of the hydride surface by the reaction product HBr or, possibly, by Br_2. Previous experience with this hydride demonstrates that it is readily deactivated by small amounts of HI or I_2.

This observation provides further evidence, this time in a straightforward neutral-neutral reaction, that CF_3Br reacts with atomic hydrogen yielding the relatively unreactive product HBr. Much more work remains to establish relative yields and reaction rates. Consequently, they are not addressed in this study.

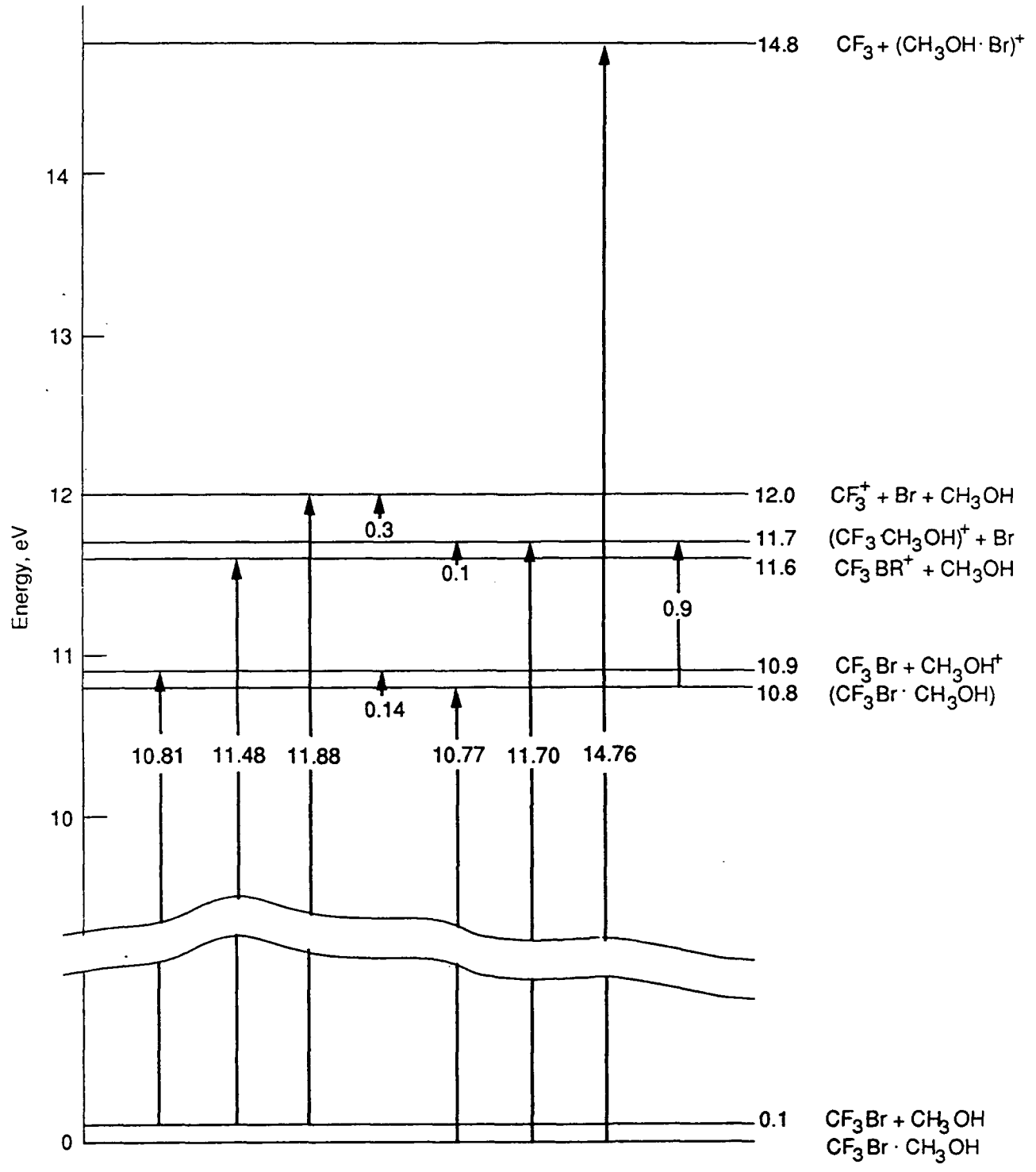

Figure 25. Energy Diagram for Neutral and Ionic Species in $CF_3Br + CH_3OH$ System.

E. KINETIC ENERGY ANALYZER

The kinetic energy analyzer was tested by photoionization of O_2 and CO_2. First, a mixture of O_2 in He (1:23) was photoionized at 700Å, and the kinetic energy distribution of O_2^+ was determined (Figure 26). The curve shows that O_2^+ produced by direct ionization has an energy in the molecular beam of about 0.4 eV and a width (full width at half maximum height, FWHM) of about 0.15 eV. Both of these values are close to those expected.

Next, O^+ from the dissociative ionization event

$$O_2 + h\upsilon \rightarrow O^+ + O + e \qquad [6]$$

was analyzed for kinetic energy distribution for various photon energies above the known threshold for this process (Figure 27). Complete analysis of these results requires deconvolution of the beam function and the ion-yield function. Though a thorough analysis cannot be presented, it is evident that with greater internal energy in the metastable excited ion $(O_2^+)^*$ produced by direct ionization, the average energy of O^+ increases and the distribution broadens dramatically to higher energy. Detailed analysis of this example is important because Reaction [6] is kinematically determined; no energy can be disposed of as internal energy in either product O^+ or O.

A singular experiment was conducted using CO_2 instead of O_2. Kinetic energy distributions of ions in both processes

$$CO_2 + h\upsilon \rightarrow CO_2^+ + e$$

and

$$CO_2 + h\upsilon \rightarrow OC + O^+ + e$$

were determined from a 500-torr expansion of a 1:19 mixture of CO_2 in He. The results for ionization of 636 Å are shown in Figure 28. As in the case of O^+ from O_2, the O^+ energy distribution at about 0.3 eV above threshold is much broader than the threshold

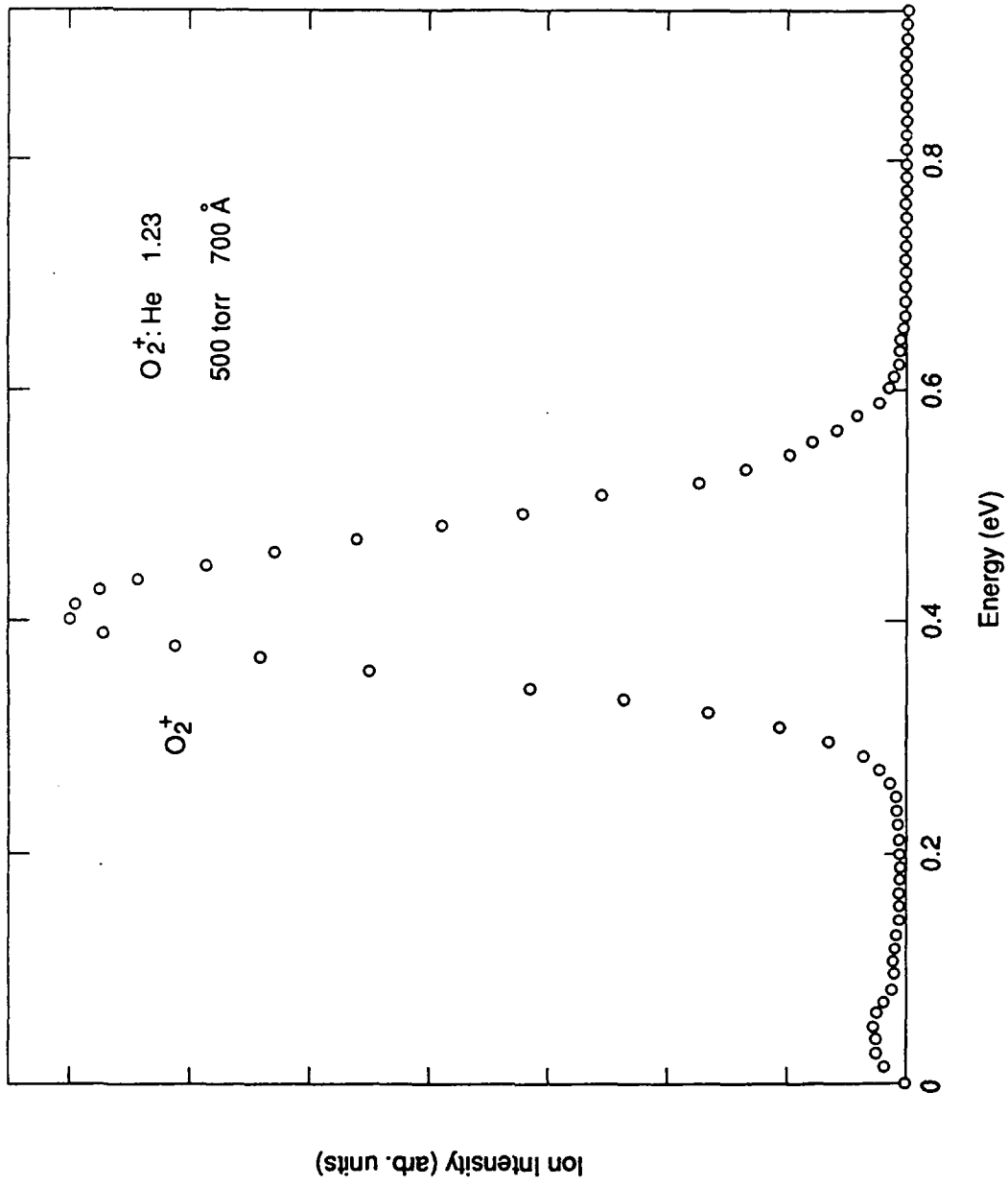

Figure 26. Kinetic Energy Distribution of O_2 in He at a Nozzle Stagnation Pressure of 500 Torr.

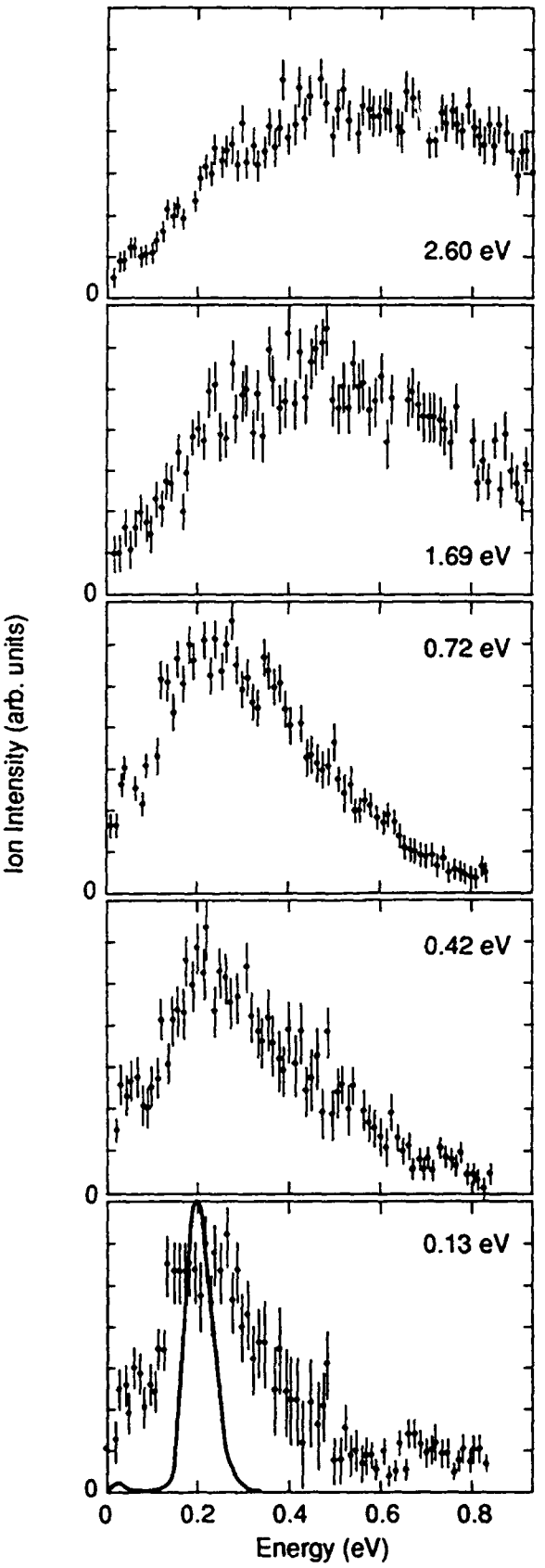

Figure 27. Kinetic Energy Distributions of O^+ from O_2 by Photoionization. (The energies in the panels are the incident photon energies above the threshold for this reaction. The solid line in the bottom panel is the distribution expected at threshold (0.00 eV).)

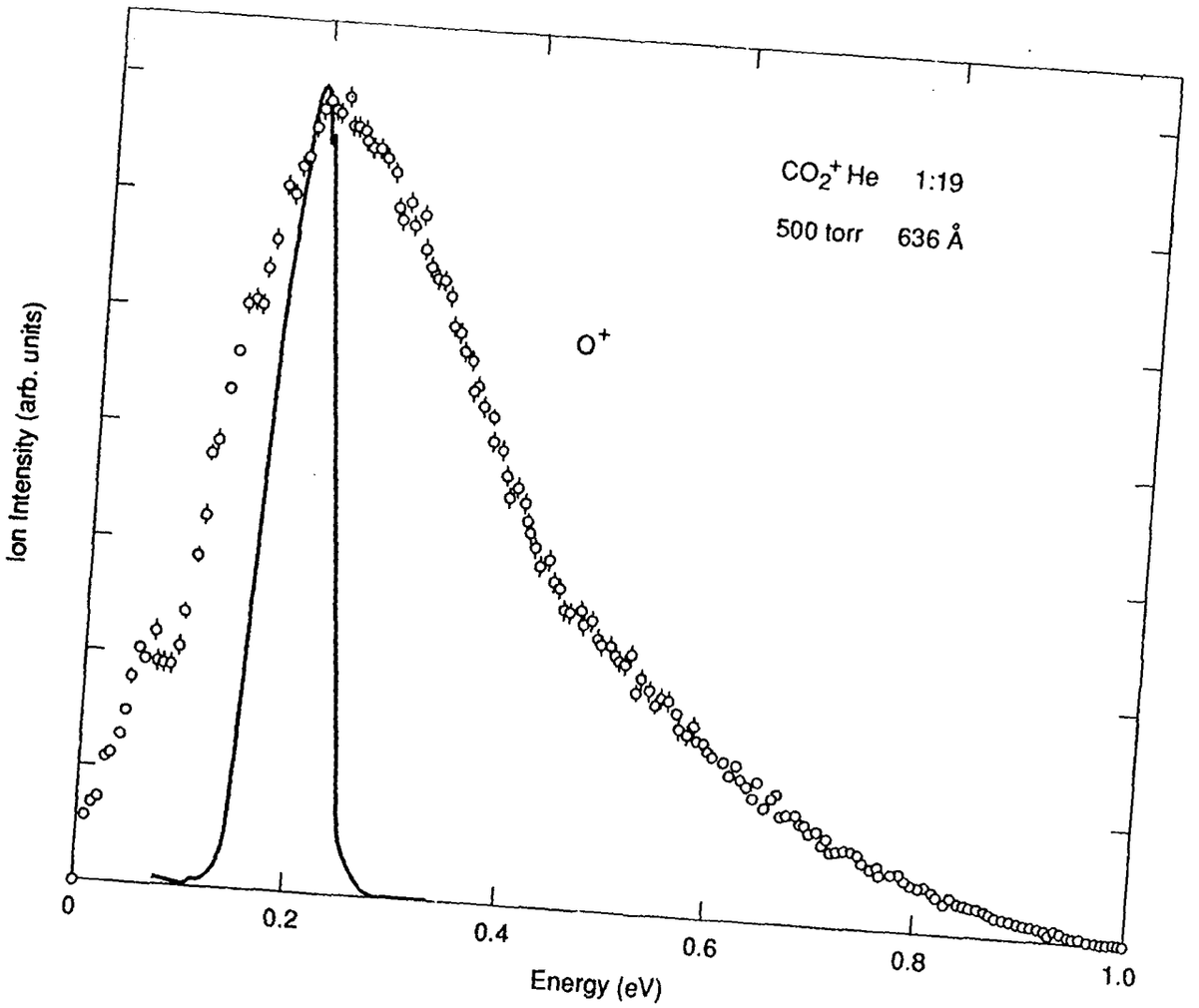

Figure 28. Kinetic Energy Distribution of O^+ from CO_2 Taken in a 500-torr Nozzle Expansion of 1:19 CO_2 in He at 636 Å. (The solid line is the distribution at 0.00 eV above the threshold for this process.)

measurement. In the case of CO_2, it is possible for some energy to be disposed of as internal energy in the CO product molecule.

A single example of extension of the fragment ion kinetic energy measurements to clusters illustrates the potential richness of this approach.

In Figure 29 the kinetic energy distribution of $C_4H_6^+$ (1,3-butadiene cation), from $C_4H_6 \cdot SO_2$ formed in a 1:2.3 mixture of C_4H_6 in SO_2, is shown at the ionization threshold of $C_4H_6 \cdot SO_2$. The peak is centered at about 0.13 eV and has a width of ~ 0.07 eV. Note that the signal drops to baseline abruptly after the $C_4H_6^+$ peak is passed. This is demanded by the fact that very little excess energy is available above the $C_4H_6^+$ production threshold. On the other hand, if the kinetic energy distribution of $C_4H_6^+$ is measured at incident photon energy of 600Å (20.66 eV), the results in Figure 30 are obtained. At this energy, the peak shape is quite different from that in the vicinity of the threshold. In addition to having distinct low-energy features, the signal gradually drops so that there are measurable $C_4H_6^+$ ions with 0.9 eV kinetic energy. Furthermore, the fragment $C_4H_6SO^+$ from $C_4H_6 \cdot SO_2$ in the same expansion and at the same ionization energy, 600 Å = 20.66 eV, has a vastly different kinetic energy distribution (Figure 31). Questions arise as to the reasons for the strange peak shapes observed at 600 Å. It is expected that careful analysis of these examples would give insight into the dissociative photoionization mechanisms. In conclusion, it would be revealing to apply this approach to the $CF_3Br \cdot CH_3OH$ system.

F. ENERGY TRANSFER BETWEEN DIOXYGEN AND HYDROCARBONS

Three complexes with molecular oxygen have been studied: $C_6H_6 \cdot O_2$, $C_6F_6 \cdot O_2$, and $CF_3Br \cdot O_2$. The IP of the organic moiety lies 2.81, 2.09, and 6.56 eV below the IP of O_2, respectively. In our experience the lowest IP moiety in weakly-bound complexes typically serves as the chromophore for the incident photon in single photon ionization events. Thus, in the first two systems (with large ΔIP values), energy transfer is expected to be from the organic portion to molecular oxygen. In both complexes, once the newly formed organic ion, $C_6H_6^+$ or $C_6F_6^+$, has enough energy above its ground state to

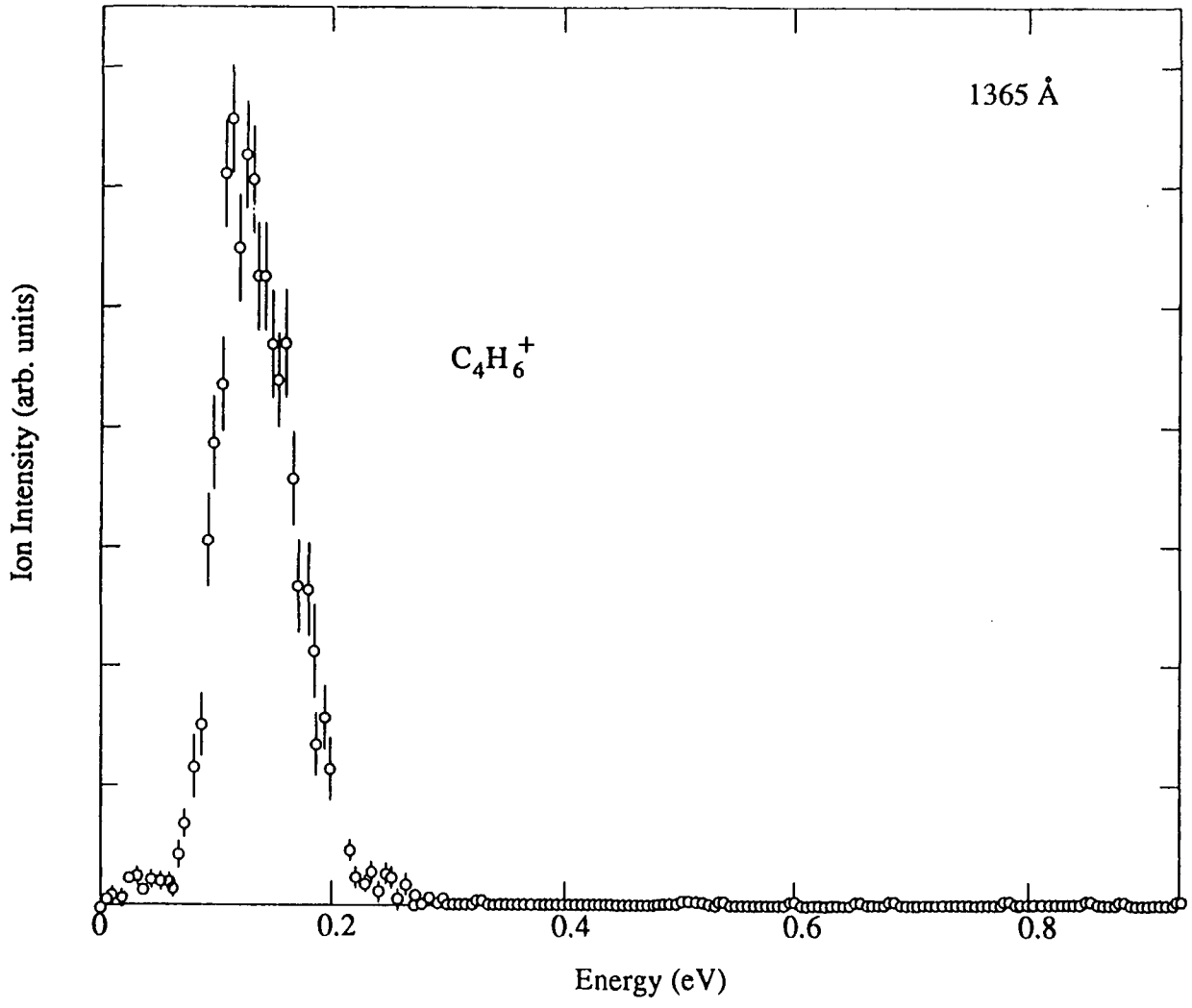

Figure 29. Kinetic Energy Distribution of $C_4H_6^+$ from $C_4H_6 \cdot SO_2$ at an Ionization Energy of 1365 Å (9.08 eV).

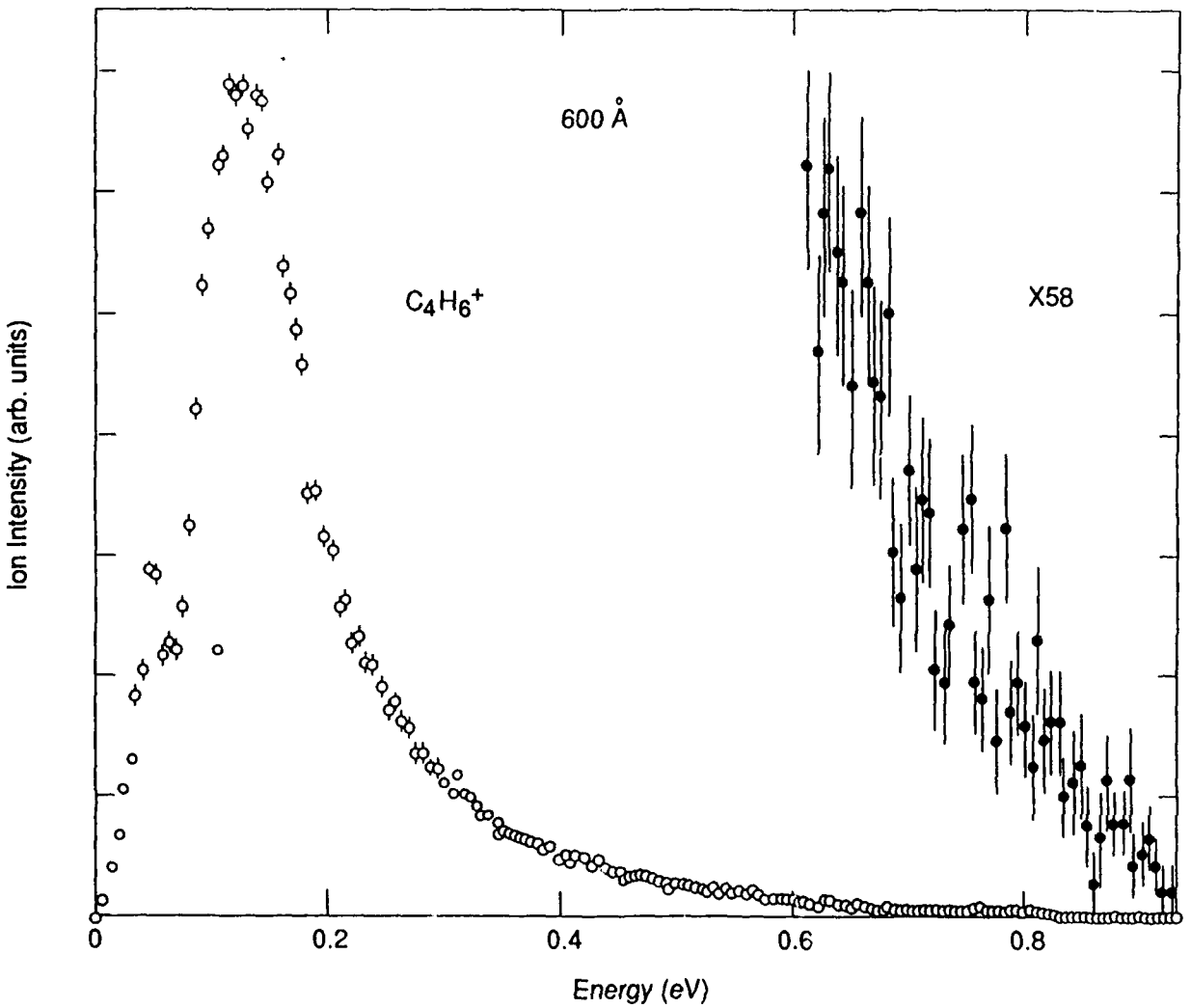

Figure 30. Kinetic Energy Distribution of $C_4H_6^+$ from C_4H_6•SO_2 at an Ionization Energy of 600 Å (20.66 eV).

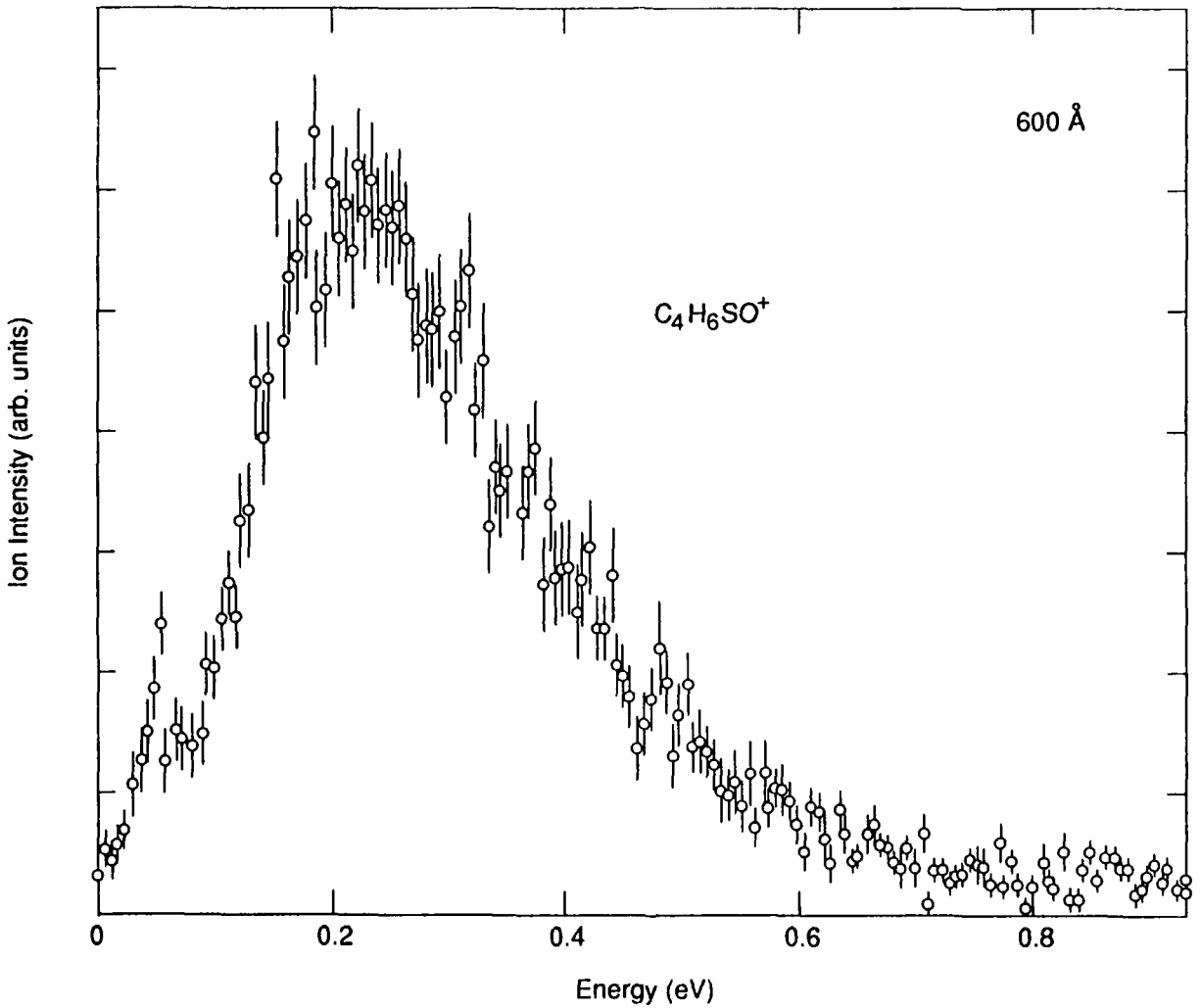

Figure 31. Kinetic Energy Distribution of $C_4H_6^+$ from $C_4H_6 \cdot SO_2$ at an Ionization Energy of 600 Å (20.66 eV).

dissociate the dioxygen bound to it, energy is transferred, cleaving the O_2 bond and leaving the fragment ion $C_6H_6O^+$ or $C_6F_6O^+$.

In the case of $CF_3Br{\bullet}O_2$ however, ΔIP is small, 0.56 eV, and the results are dramatically different. The yield of $CF_3Br{\bullet}O_2^+$ is very low and does not increase substantially as the photon energy increases. The PIE does not show the characteristic spike about 0.5 eV above threshold that we identify with fragmentation of CF_3Br^+ into CF_3^+ and Br. It appears that ionization occurs by absorption of a photon by the O_2 moiety producing either a Rydberg state or the ion, and instead of intracluster Penning ionization occurring, the most probable event is simple dissociation into CF_3Br and O_2^+. A small amount remains as $CF_3Br{\bullet}O_2^+$. The dissociative ionization product CF_3BrO^+ is not detected. From this we conclude that transfer of electronic excitation energy from dioxygen to CF_3Br in a collision does not efficiently produce CF_3Br^+, CF_3^+ + Br, or CF_3 + Br. Therefore, the mechanism for injecting Br atoms into a flame by electronic energy transfer from dioxygen is highly unlikely.

SECTION V
CONCLUSIONS AND RECOMMENDATIONS

A. CONCLUSIONS

This study has provided informative insights into the reactions between the fire extinguishant CF_3Br and the dominant flame free radicals H, O, and OH. The most important conclusions are given below:

(1) Little evidence that CF_3Br interacts with either O or OH radicals has been found. Potential fire extinguishants are compounds that will trap either of these radicals efficiently.

(2) The very low C-Br bond energy in the CF_3Br^+ ion suggests that some Br may enter flames from CF_3Br^+. The means of forming CF_3Br^+ or similar cations in flames should be explored.

(3) CF_3Br has been shown to react with H atoms. This reaction is found in the case of dissociative photoionization of clusters and in the metal hydride reduction of CF_3Br.

(4) Kinetic energy distributions of fragment ions of dissociative photoionization events can be measured. Detailed analysis of the results may show how to apply the method to systems involving halons.

(5) Since the high stability of and thermodynamic preference for CF_3^+ may be a strong driving force in the extinguishment process, a more thorough examination of the extinguishment mechanism should be conducted.

(6) Small heteroclusters can be prepared in supersonic nozzle expansions and the relative number densities of the neutrals can be determined.

(7) Analysis of clusters in a ternary molecular beam has been carried out for the first time.

(8) Cluster growth in free jet expansions cannot be described by a model based on near-equilibrium processes.

(9) Studies of frozen collision complexes, i.e., weakly bound or van der Waals complexes, offer a powerful method for learning about initial steps of reaction chemistry.

This approach should continue to yield worthwhile information about the mechanisms of reactions of halons, CFCs, HCFCs, and other small molecules.

B. RECOMMENDATIONS

The results of the experiments reported in this study have some potentially significant implications for identification of alternative fire suppression agents. Among the new concepts are the following:

(1) Since it appears possible that ions of extinguishers may be extremely important, a search for compounds with lower ionization potential than CF_3Br and possessing a weak C-Br (or C-X, where X is a halogen or other leaving group) bond in the ion should be conducted. It is likely that such compounds will have relatively short tropospheric lifetimes, thus contributing to reduced ODP and GWP.

(2) A search for compounds that trap either O or OH radicals should be conducted. For example, a molecule such as CF_3CH_2ONO will decompose readily at flame temperatures to give CF_3, CH_2O, and NO. NO reacts with either O or OH and may therefore serve as the radical trap, turning off the flame propagation step. Furthermore, this class of compounds should have short atmospheric lifetimes. The toxicity questions, however, remain. Other families of compounds with similar chemical properties exist, e.g., substituted hydroperoxides, and should be investigated.

(3) Since these results point to the importance of a very stable carbonium ion, CF_3^+ in this case, a search should be conducted for molecules containing other groups that can form stable carbonium ions (e.g., allylic, tertiary, or benzylic groups).

REFERENCES

1. Walters, E. A., Nimitz, J. S., Tapscott, R. E., Brabson, G. D. May, J. H., Clay, J. T., Jr., Arneberg, D. L., Wall, M. H., Beeson, H. D., and Moore, T. A., Initial Fire Suppression Reactions of Halons Phase II -- Verification of Experimental Approach and Initial Studies, ESL-TR-89-50, Vol. 2 of 3, Air Force Engineering and Services Center, Tyndall Air Force Base, Florida, August 1989.

2. Walters, E. A., Grover, J. R., Tapscott, R. E., Clay, J. T., Jr., Arneberg, D. L., Wall, M. H., Nimitz, J. S., and Beeson, H. D., Initial Fire Suppression Reactions of Halons Phase III -- Molecular Beam Experiments Involving Halon Clusters, ESL-TR-89-50, Vol. 3 of 3, Air Force Engineering and Services Center, Tyndall Air Force Base, Florida, September 1989.

3. Grover, J. R., Walters, E. A., Arneberg, D. L., and Santandrea, C. J., "Competitive Production of Weakly Bound Heterodimers in Free Jet Expansions," Chemical Physics Letters, Vol. 146, p. 305-309, 1988.

4. Grover, J. R., Walters, E. A., Newman, J. K., and White, M. G., "Measurement of Dissociation Energies of Gas Phase Neutral Dimers by a Photoionization Technique: Values for *trans*-2-Butene/Sulfur Dioxide, (*trans*-2-Butene)$_2$, and Benzene/Sulfur Dioxide," Journal of American Chemical Society, Vol. 107, p. 7329-7339, 1985.

5. Grover, J. R., and Walters, E. A., "Optimization of Weak Neutral Dimers in Nozzle Beams," Journal of Physical Chemistry, Vol. 90, p. 6201-6210, 1986.

6. Benson, S.W., Thermochemical Kinetics, Wiley and Sons, New York, 1976.

7. Stull, D. R., and Prophet, H., eds., JANAF Thermochemical Tables, 2nd ed., National Bureau of Standards, 1971.

8. Grover, J. R., Herron, W. J., Coolbaugh, M. T., Peifer, W. R., and Garvey, J. F., Chemical Physics Letters, 1991, draft in preparation.

9. Buck, U., Gu, X. J., Lauenstein, C., and Rudolph, A., "Infrared Photodissociation of Size-Selected Methanol Clusters," Journal of Chemical Physics, Vol. 92, p. 6017-6029, 1990.

10. Walters, E. A., Grover, J. R., Arneberg, D. L., Clay, J. T., and Wall, M. H., "Photoionization Studies in the CF_3Br+O_2 System," American Chemical Society, 199th National Meeting, Boston, MA, April 1990, Abstract PHYS-260.

11. Odutola, J. A., Viswanathan, R., and Dyke, T. R., "Molecular Beam Electric Deflection Behavior and Polarity of Hydrogen-Bonded Complexes of ROH, RSH, and RNH," Journal of the American Chemical Society, Vol. 101, p. 4787-4792, 1979.

12. Cook, K. D., Jones, G. G., and Taylor, J. W., "A Photoionization Study of Hydrogen-Bound Clusters in a Supersonic Molecular Beam," International Journal of Mass Spectromotry and Ion Physics, Vol. 35, p. 273-292, 1980.

13. Hoffbauer, M. A., Giese, C. F., and Gentry, W. R., "Infrared Photodissociation of Methanol Dimers," Journal of Physical Chemistry, Vol. 88, p. 181-184, 1984.

14. Olesik, S. V., and Taylor, J. W., "Unimolecular Fragmentation Pathways of Methanol, Ammonia, and Water Neutral Clusters," International Journal of Mass Spectrometric Ion Processes, Vol. 57, p. 315-327, 1984.

15. Mori, Y., and Kitagawa, T., "Mass Spectrometric Studies on Hydrogen-Bonded Clusters Produced via Supersonic Expansions Characteristic Ions for Detection of $(H_2O)n$, $(CH_3OH)n$ and $(C_2H_5OH)n(n\leq4)$," Chemical Physics Letters, Vol. 128, pp. 383-388, 1986.

16. Huisken, F., and Stemmler, M., "Infrared Photodissociation of Small Methanol Clusters," Chemical Physics Letters, Vol. 144, p. 391-395, 1988.

17. Stace, A. J., and Shukla, A. K., "Preferential Solvation of Hydrogen Ions in Mixed Clusters of Water, Methanol, and Ethanol," Journal of the American Chemical Society, Vol. 104, p. 5314-5322, 1982.

18. Hager, J., Ivanco, M., Smith, M. A., and Wallace, S. C., "Two-Color Threshold Photoionization Spectroscopy of Jet-Cooled Indole Clusters," Chemical Physics, Vol. 105, p. 397-416, 1986.

19. Stace, A. J., "Chemical Reactions on Clusters. 5. Gas-Phase Unimolecular Decomposition of the CH_3OH, CH_3OD, CD_3OH, and CD_3OD Ions in Association with Argon and Carbon Dioxide Clusters," Journal of Physical Chemistry, Vol. 91, p. 1509-1515, 1987.

20. Crooks, J., Stace, A. J., and Whitaker, B. J., "Infrared Laser Study of Methanol, Ethanol, and SF_6 Solvation in Water Clusters," Journal of Physical Chemistry, Vol. 92, p. 3554-3560, 1988.

21. Klemperer, W., Yaron, D., and Nelson, Jr., D. D., "Metastability and Cooling Timescales of Molecular Complexes," Faraday Discussions of the Chemical Society, Vol. 86, p. 261-267, 1988.

22. Amirav, A., Even, U., and Jortner, J., "Microsopic Solvation Effects on Excited-State Energetics and Dynamics of Aromatic Molecules in Large Van der Waals Complexes," Journal of Chemical Physics, Vol. 75, p. 2489-2512, 1981.

23. Curtiss, L. A., and Blander, M., "Thermodynamic Properties of Gas-Phase Hydrogen-Bonded Complexes," Chemical Reviews, Vol. 88, p. 827-841, 1988.

24. Walters, E. A., Grover, J. R., and White, M. G., "A Photoionization Study of the Van der Waals Molecule $C_2H_4 \bullet HCl$," Zeitsthrift fur Physik, D 4, p. 103, 1986.

25. Grover, J. R., Walters, E. A., Newman, J. K., and White, M. G., "Photoionization Studies of Internally Reactive Small Clusters: Van der Waals Complexes of 1,3-Butadiene with Sulfur Dioxide," Journal of the Americal Chemical Society, Vol. 112, p. 6499-6506, 1990.

26. Grover, J. R., Walters, E. A., and Hui, E. T., "Dissociation Energies of the Benzene Dimer and Dimer Cation," Journal of Physical Chemistry, Vol. 91, p. 3233-3237, 1987.

27. Walters, E. A., Grover, J. R., White, M. G., and Hui, E. T., "On the Structure and Thermochemistry of the Van der Waals Molecule $C_6H_6 \bullet HCl$ and its Photoion $(C_6H_6 \bullet HCl)^+$," Journal of Physical Chemistry, Vol. 89, p. 3814-3818, 1985.

28. Grover, J. R., Hagneow, G., and Walters, E. A., "Complexes of O_2 with Hydrocarbons and Fluorocarbons," Annual Report BNL-52218, National Synchrotron Light Source, p. 199, 1989.

(The reverse side of this page is blank.)